The CLIC detector and physics study

Philipp Roloff (CERN)
on behalf of the CLIC detector and physics study

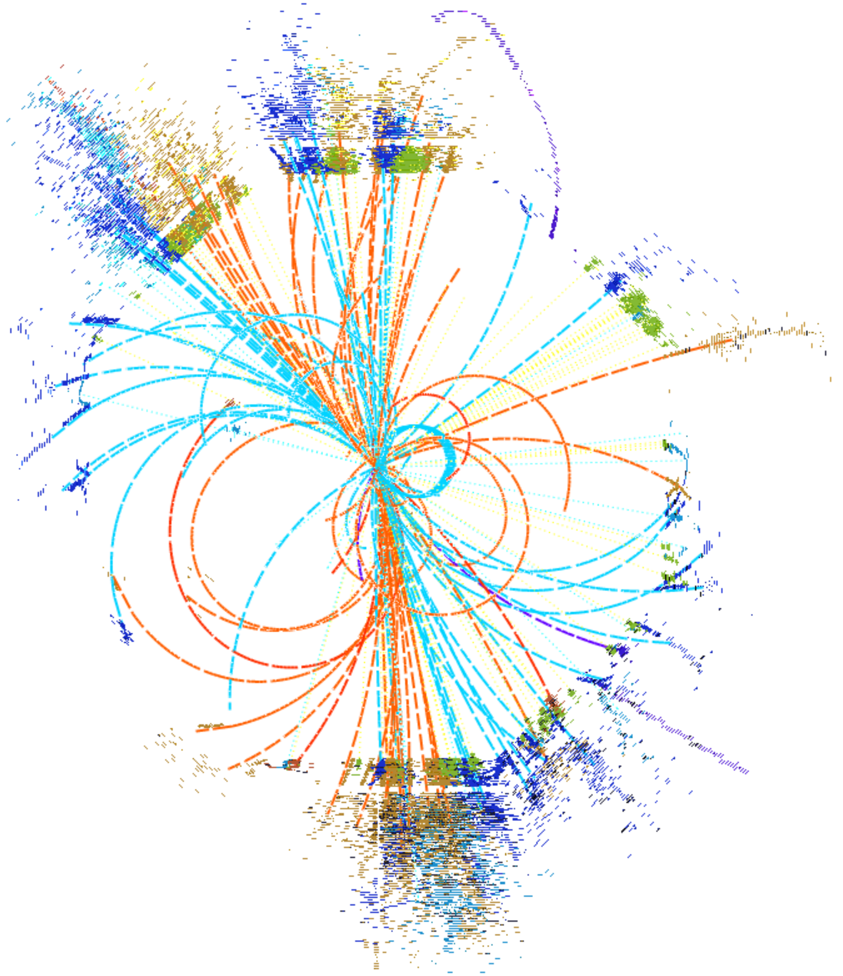

ILC & more miniworkshop, Como, 17/05/2013

The CLIC detector and physics study

- Pre-collaboration structure based on “Memorandum of Cooperation” (MoC): http://lcd.web.cern.ch/lcd/Home/MoC.html
- CERN acts as host laboratory
- At the moment 17 institutes from 14 countries, more contributors most welcome!

CLIC detector R&D as part of the LC work

CALICE
Calorimeter for ILC

LC TPC

FCAL
Collaboration
High precision design

SiD

clic

ilcILD.org

AIDA

The CLIC CDR

The CLIC CDR was published in 2012:

- **Volume 1:** A Multi-TeV Linear Collider based on CLIC Technology, CERN-2012-005, http://cds.cern.ch/record/1500095
- **Volume 2:** Physics and Detectors at CLIC, CERN-2012-003, http://cds.cern.ch/record/1425915
- **Volume 3:** The CLIC Programme: towards a staged e^+e^- Linear Collider exploring the Terascale, CERN-2012-005, http://cds.cern.ch/record/1475225

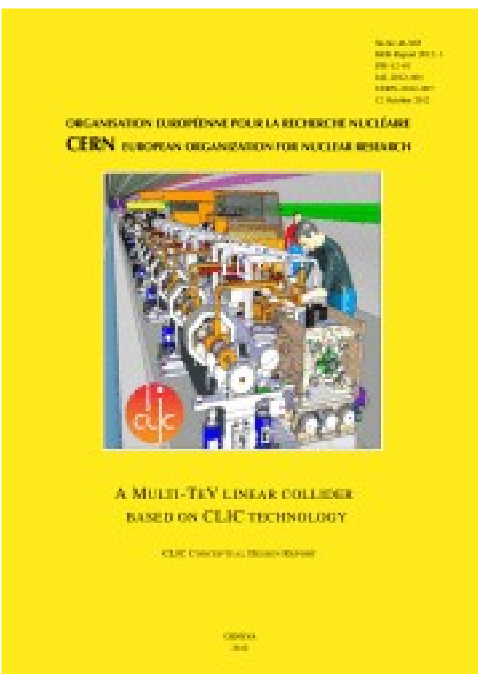

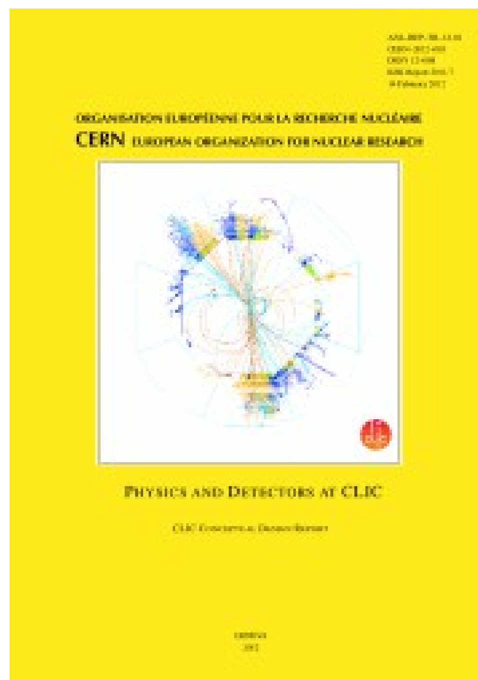

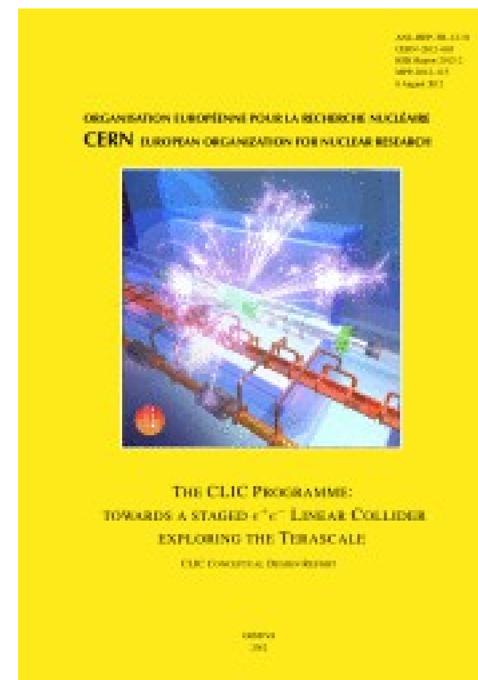

Selected CLIC parameters

	CLIC at 3 TeV
L ($cm^{-2}s^{-1}$)	$5.9 \cdot 10^{34}$
Bunch separation	0.5 ns
#Bunches / train	312
Train duration	156 ns
Train rep. rate	50 Hz
Crossing angle	20 mrad
Particles / bunch	$3.72 \cdot 10^{9}$
σ_x/σ_y (nm)	≈ 45 / 1
σ_z (μm)	44

Drive timing requirements for CLIC detector

Very small beam profile at the interaction point

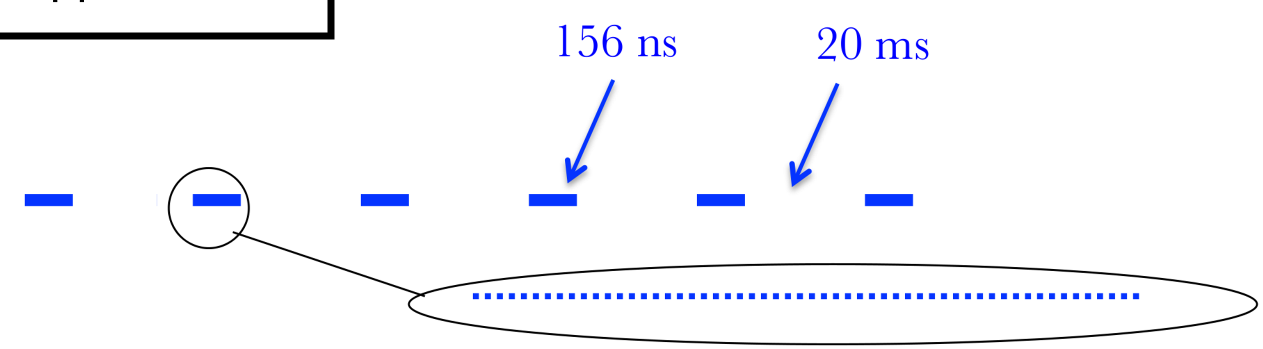

CLIC: trains at 50 Hz, 1 train = 312 bunches, 0.5 ns apart

Luminosity spectrum

Significant energy loss at the interaction point due to Beamstrahlung

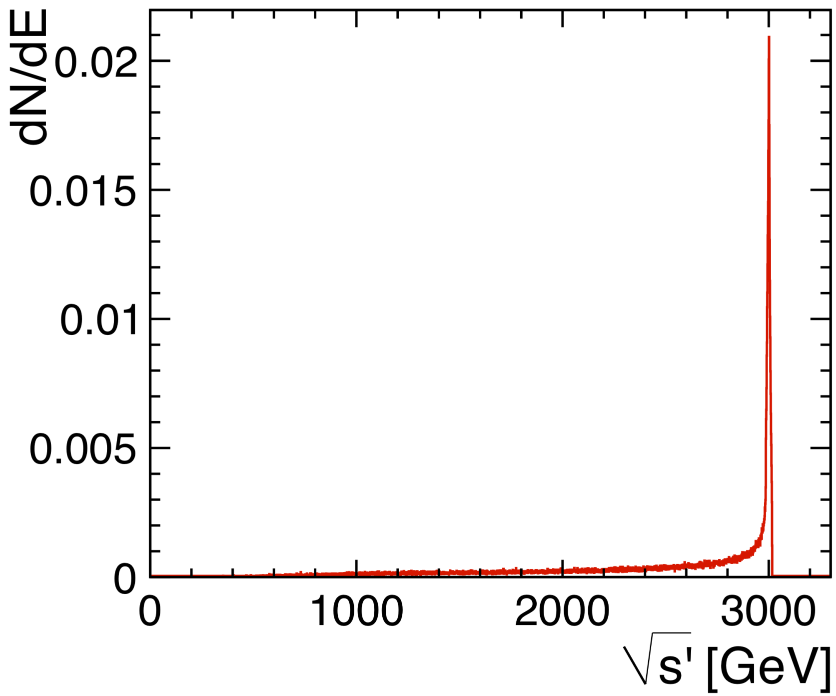

$$\sqrt{s'} = \sqrt{4 \cdot E_1 \cdot E_2}$$

Full luminosity: $L = 5.9 \cdot 10^{34}\ cm^{-2}s^{-1}$
In the most energetic 1%:
("peak luminosity") $L_{0.01} = 2.0 \cdot 10^{34}\ cm^{-2}s^{-1}$

Most physics processes are studies well above the production threshold
→ Profit from (almost) full luminosity

Beam related backgrounds

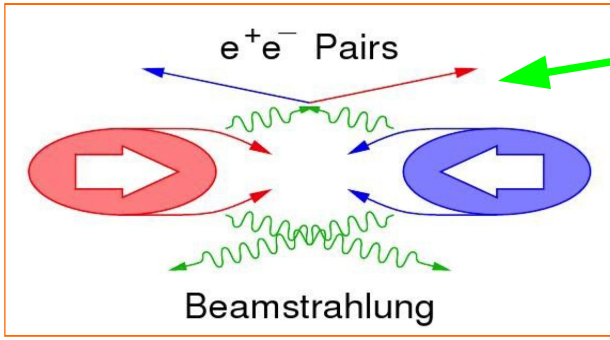

- e^+e^- pairs
- $\gamma\gamma \rightarrow$ hadrons
- Beam halo muons

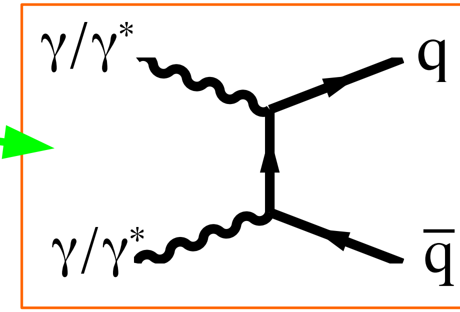

Coherent e^+e^- pairs:
$7 \cdot 10^8$ per BX, very forward
Incoherent e^+e^- pairs:
$3 \cdot 10^5$ per BX, rather forward
→ Detector design issue
(high occupancies)

γγ → hadrons
- "Only" 3.2 per BX at 3 TeV
- Main background

in calorimeters and trackers
→ Impact on physics

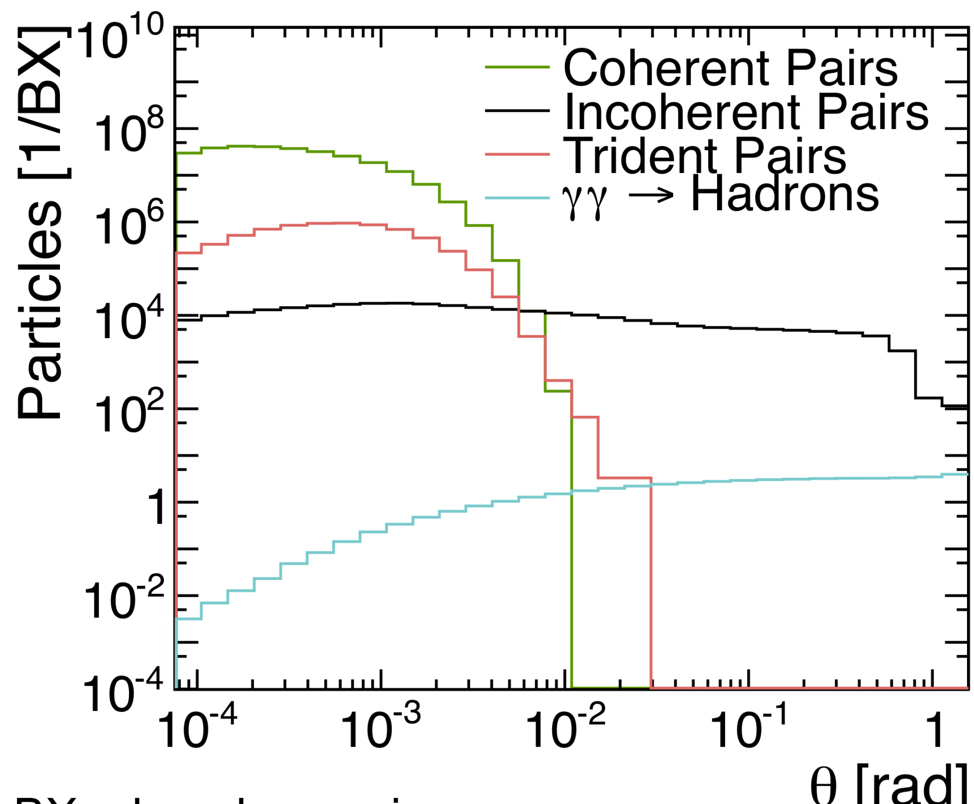

BX = bunch crossing

CLIC physics potential

Advantage of e^+e^- collisions:

- Defined initial state
- Precision measurements possible due to clean conditions
- Well suited for weakly interacting states (e.g. sleptons, gauginos)
- Polarised (electron) beam

→ **Complementary / enhanced discovery reach compared to the LHC**

Examples highlighted in the CDR:

- Higgs physics (SM and non-SM)
- Top physics
- SUSY
- Higgs strong interactions
- Z'
- Contact interactions
- Extra dimensions
- …

Higgs production at CLIC

At 350 GeV: Mostly HZ, allows to reconstruct Higgs from recoil mass

At higher energies:

- WW fusion dominates, high number of Higgs bosons
- ZZ fusion about an order of magnitude smaller
- The extraction of the Higgs self-coupling from $HH\nu\bar{\nu}$ becomes possible

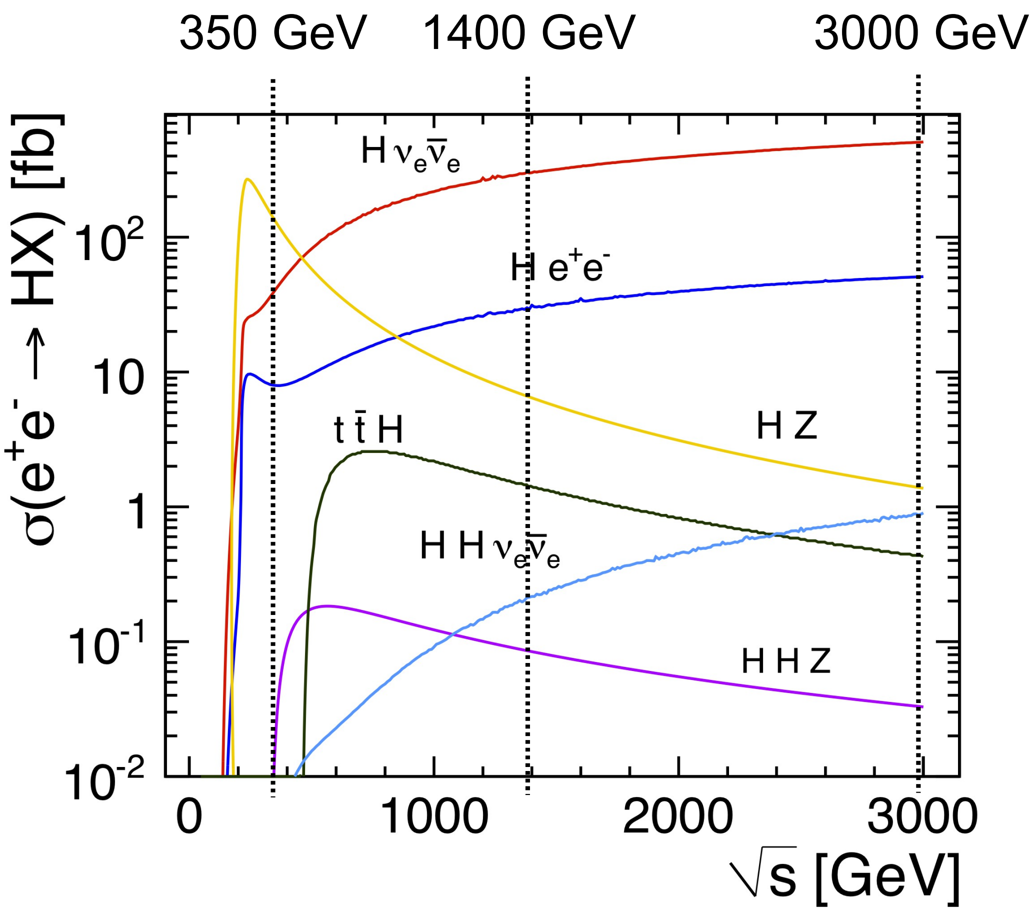

1.4 TeV: Suitable to measure the top Yukawa coupling using $t\bar{t}H$ events

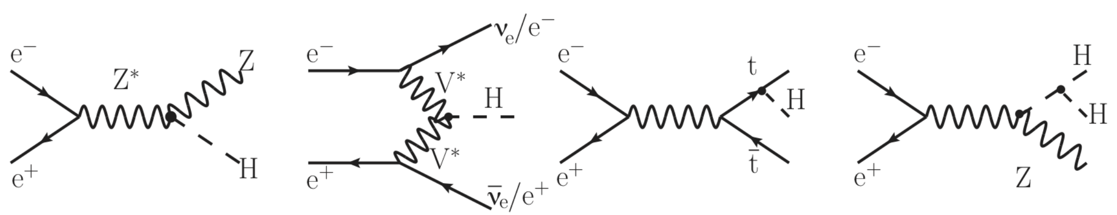

Higgs benchmark results

Energy	Observable	Precision
350 GeV	σ(HZ)	4%
	mass (from recoil)	120 MeV
	σ x BR(H → $\tau^+\tau^-$)	5.7%
500 GeV	σ(HZ) / σ(H$\nu\bar{\nu}$)	5%
	mass	100 MeV
1.4 TeV	σ x BR(H → $\tau^+\tau^-$)	<3.7%
	self-coupling λ	30%
	σ(ttH)	≈8% (estimated from ILC study at 1 TeV)
3 TeV	σ x BR(H → $b\bar{b}$)	0.2%
	σ x BR(H → $c\bar{c}$)	3.2%
	σ x BR(H → $\mu^+\mu^-$)	15%
	self-coupling λ	16%

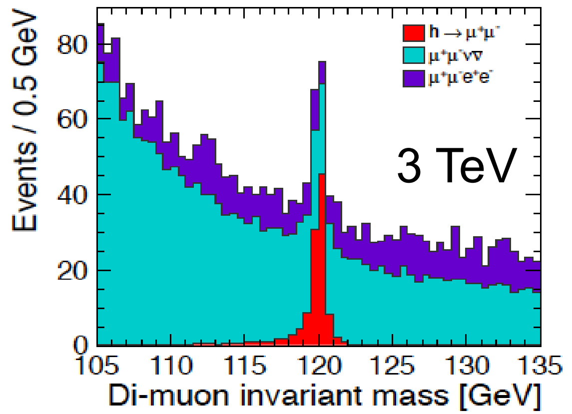

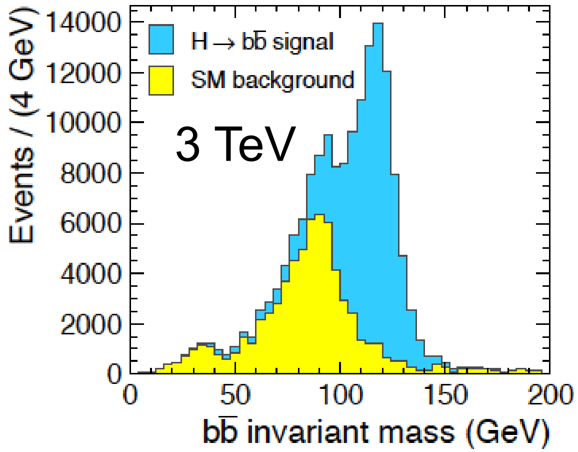

• All results based on full detector simulations (Geant4) and considering pileup from beam-induced backgrounds

• All results for unpolarised beams, σ(H$\nu\bar{\nu}$) and σ(HH$\nu\bar{\nu}$) about 80% larger for -80% polarisation of the electron beam

CLIC physics performance for the SM Higgs

Ongoing effort to investigate the full physics performance of CLIC for SM Higgs boson measurements at 350, 1400 and 3000 GeV:

350 GeV:
- Model-independent mass and cross section from recoil method
- $H \to b\bar{b}$, $H \to c\bar{c}$, $H \to gg$, $BR(H \to \tau^+\tau^-)$, $H \to WW^*$

1.4 GeV:
- $H \to b\bar{b}$, $H \to c\bar{c}$, $H \to gg$, $BR(H \to \tau^+\tau^-)$, $H \to WW^*$, $H \to Z\gamma$, $H \to \gamma\gamma$, $H \to \mu^+\mu^-$
- top Yukawa coupling from the $t\bar{t}H$ cross section
- Higgs self-coupling from $HH\nu\bar{\nu}$ cross section (improvements by refined analysis expected)
- Higgs production in ZZ-fusion

3 TeV:
- $H \to b\bar{b}$, $H \to c\bar{c}$, $H \to gg$, $H \to WW^*$, $H \to \mu^+\mu^-$
- Higgs self-coupling from $HH\nu\bar{\nu}$ cross section (improvements by refined analysis expected)

In addition:
- Extraction of the Higgs width at all energies
- Extraction of the Higgs couplings from combined fit to all measurements

Expect full set of results in the summer

SUSY benchmark scenarios

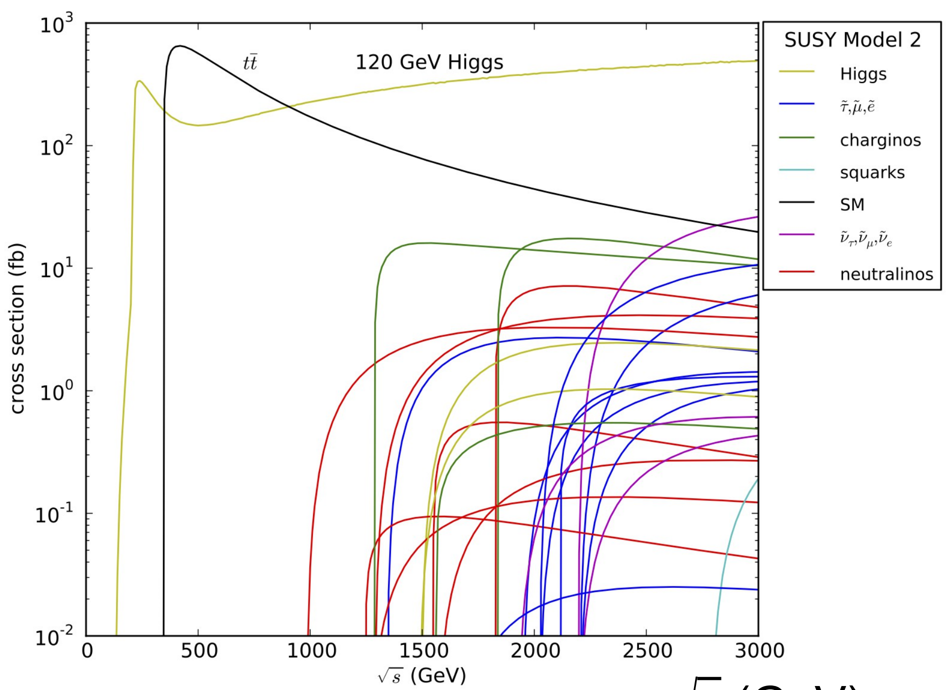

$\sqrt{s}$ (GeV)

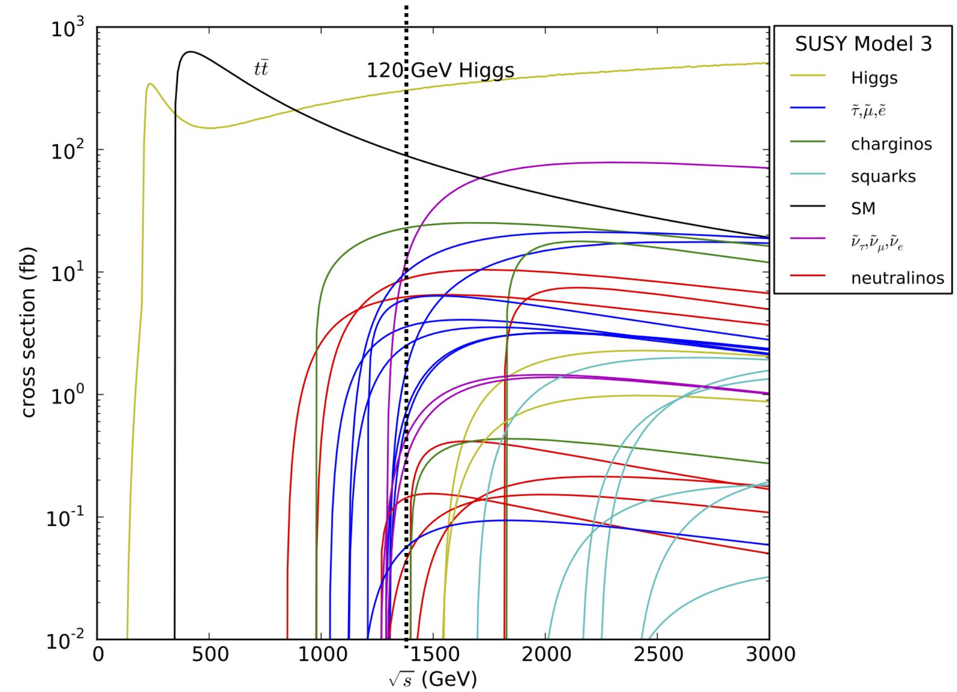

$\sqrt{s}$ (GeV)

One of the two models investigated at 3 TeV

Model investigated at 1.4 TeV: sleptons and light gauginos accessible

SUSY benchmark studies at 1.4 TeV

$\sqrt{s}$ (TeV)	Process	Decay mode	SUSY model	Measured quantity	Unit	Generator value	Stat. error
1.4	Sleptons production	$\tilde{\mu}_R^+\tilde{\mu}_R^- \to \mu^+\mu^-\tilde{\chi}_1^0\tilde{\chi}_1^0$	III	σ	fb	1.11	2.7%
				$\tilde{\ell}$ mass	GeV	560.8	0.1%
				$\tilde{\chi}_1^0$ mass	GeV	357.8	0.1%
		$\tilde{e}_R^+\tilde{e}_R^- \to e^+e^-\tilde{\chi}_1^0\tilde{\chi}_1^0$		σ	fb	5.7	1.1%
				$\tilde{\ell}$ mass	GeV	558.1	0.1%
				$\tilde{\chi}_1^0$ mass	GeV	357.1	0.1%
		$\tilde{\nu}_e\tilde{\nu}_e \to \tilde{\chi}_1^0\tilde{\chi}_1^0 e^+e^-W^+W^-$		σ	fb	5.6	3.6%
				$\tilde{\ell}$ mass	GeV	644.3	2.5%
				$\tilde{\chi}_1^\pm$ mass	GeV	487.6	2.7%
1.4	Stau production	$\tilde{\tau}_1^+\tilde{\tau}_1^- \to \tau^+\tau^-\tilde{\chi}_1^0\tilde{\chi}_1^0$	III	$\tilde{\tau}_1$ mass	GeV	517	2.0%
				σ	fb	2.4	7.5%
1.4	Chargino production	$\tilde{\chi}_1^+\tilde{\chi}_1^- \to \tilde{\chi}_1^0\tilde{\chi}_1^0 W^+W^-$	III	$\tilde{\chi}_1^\pm$ mass	GeV	487	0.2%
				σ	fb	15.3	1.3%
	Neutralino production	$\tilde{\chi}_2^0\tilde{\chi}_2^0 \to h/Z^0 h/Z^0 \tilde{\chi}_1^0\tilde{\chi}_1^0$		$\tilde{\chi}_2^0$ mass	GeV	487	0.1%
				σ	fb	5.4	1.2%

L = 1.5 ab^{-1}

SUSY benchmark studies at 3 TeV

$\sqrt{s}$ (TeV)	Process	Decay mode	SUSY model	Measured quantity	Unit	Generator value	Stat. error
3.0	Sleptons production	$\tilde{\mu}_R^+\tilde{\mu}_R^- \to \mu^+\mu^-\tilde{\chi}_1^0\tilde{\chi}_1^0$	II	σ	fb	0.72	2.8%
				$\tilde{\ell}$ mass	GeV	1010.8	0.6%
				$\tilde{\chi}_1^0$ mass	GeV	340.3	1.9%
		$\tilde{e}_R^+\tilde{e}_R^- \to e^+e^-\tilde{\chi}_1^0\tilde{\chi}_1^0$		σ	fb	6.05	0.8%
				$\tilde{\ell}$ mass	GeV	1010.8	0.3%
				$\tilde{\chi}_1^0$ mass	GeV	340.3	1.0%
		$\tilde{e}_L^+\tilde{e}_L^- \to \tilde{\chi}_1^0\tilde{\chi}_1^0 e^+e^-hh$ $\tilde{e}_L^+\tilde{e}_L^- \to \tilde{\chi}_1^0\tilde{\chi}_1^0 e^+e^-Z^0Z^0$		σ	fb	3.07	7.2%
		$\tilde{\nu}_e\tilde{\nu}_e \to \tilde{\chi}_1^0\tilde{\chi}_1^0 e^+e^-W^+W^-$		σ	fb	13.74	2.4%
				$\tilde{\ell}$ mass	GeV	1097.2	0.4%
				$\tilde{\chi}_1^\pm$ mass	GeV	643.2	0.6%
3.0	Chargino production	$\tilde{\chi}_1^+\tilde{\chi}_1^- \to \tilde{\chi}_1^0\tilde{\chi}_1^0 W^+W^-$	II	$\tilde{\chi}_1^\pm$ mass	GeV	643.2	1.1%
				σ	fb	10.6	2.4%
	Neutralino production	$\tilde{\chi}_2^0\tilde{\chi}_2^0 \to h/Z^0 h/Z^0 \tilde{\chi}_1^0\tilde{\chi}_1^0$		$\tilde{\chi}_2^0$ mass	GeV	643.1	1.5%
				σ	fb	3.3	3.2%
3.0	Production of right-handed squarks	$\tilde{q}_R\tilde{q}_R \to q\bar{q}\tilde{\chi}_1^0\tilde{\chi}_1^0$	I	Mass	GeV	1123.7	0.52%
				σ	fb	1.47	4.6%
3.0	Heavy Higgs production	$H^0A^0 \to b\bar{b}b\bar{b}$	I	Mass	GeV	902.4	0.3%
				Width	GeV		31%
		$H^+H^- \to t\bar{b}b\bar{t}$		Mass	GeV	906.3	0.3%
				Width	GeV		27%

L = 2 ab^{-1}

Physics aims → detector needs

- **Momentum resolution**
(e.g. Higgs recoil mass, H → $\mu^+\mu^-$, leptons from BSM processes)

$$\frac{\sigma(p_T)}{p_T^2} \sim 2\times10^{-5}\,GeV^{-1}$$

- **Jet energy resolution**
(e.g. W/Z/h separation)

$$\frac{\sigma(E)}{E} \sim 3.5-5\%\ for\ E=1000-50\,GeV$$

- **Impact parameter resolution**
(b/c tagging, e.g. Higgs couplings)

$$\sigma(d_0)=\sqrt{a^2+b^2\cdot GeV^2/(p^2\sin^3\theta)},\ a\approx5\,\mu m,\ b\approx15\,\mu m$$

- **Lepton identification, very forward electron tagging**

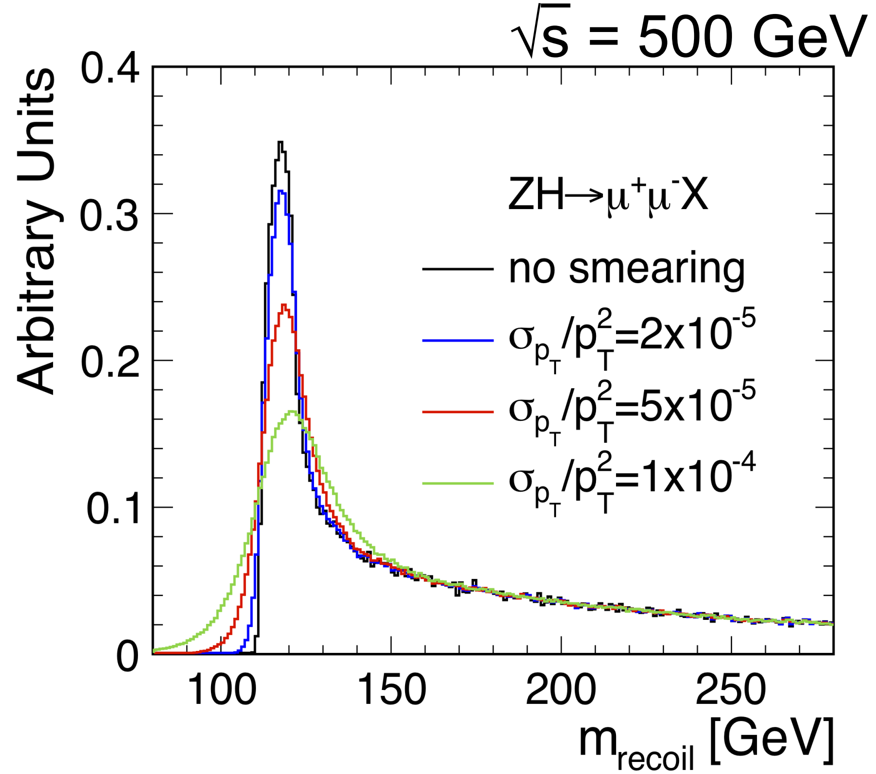

Physics aims → detector needs

- **Momentum resolution**
(e.g. Higgs recoil mass, h → $\mu^+\mu^-$, leptons from BSM processes)

$$\frac{\sigma(p_T)}{p_T^2} \sim 2\times10^{-5}\,GeV^{-1}$$

- **Jet energy resolution**
(e.g. W/Z/h separation)

$$\frac{\sigma(E)}{E} \sim 3.5-5\%\ for\ E=1000-50\,GeV$$

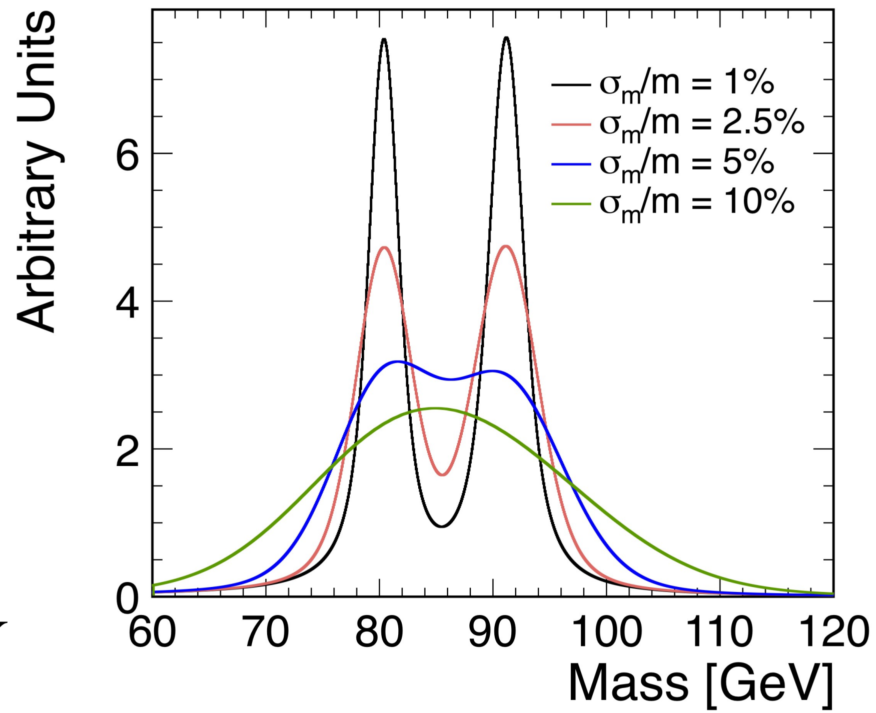

- **Impact parameter resolution**
(b/c tagging, e.g. Higgs couplings)

$$\sigma(d_0)=\sqrt{a^2+b^2\cdot GeV^2/(p^2\sin^3\theta)},\ a\approx5\,\mu m,\ b\approx15\,\mu m$$

- **Lepton identification, very forward electron tagging**

Physics aims → detector needs

- **Momentum resolution**
(e.g. Higgs recoil mass, $h \rightarrow \mu^+\mu^-$, leptons from BSM processes)

$$\frac{\sigma(p_T)}{p_T^2} \sim 2\times10^{-5}\,GeV^{-1}$$

- **Jet energy resolution**
(e.g. W/Z/h separation)

$$\frac{\sigma(E)}{E} \sim 3.5-5\%\ for\ E=1000-50\,GeV$$

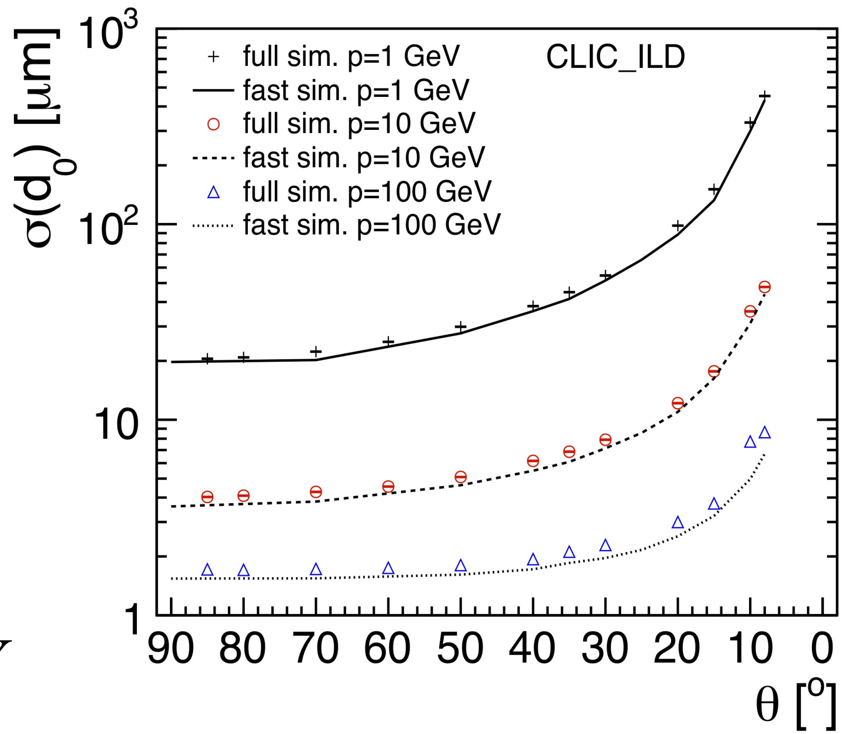

- **Impact parameter resolution**
(b/c tagging, e.g. Higgs couplings)

$$\sigma(d_0)=\sqrt{a^2+b^2\cdot GeV^2/(p^2\sin^3\theta)},\ a\approx5\,\mu m,\ b\approx15\,\mu m$$

- **Lepton identification, very forward electron tagging**

Challenges in CLIC (LC) detector R&D

These requirements lead to the following challenges:

Vertex and tracker

- Very high granularity
- Dense integration of functionalities including ≈10 ns time-stamping
- Super light materials
- Low-power design & power pulsing
- Air cooling

ultra-light

Calorimetry

- Fine segmentation in R, Φ and Z
- Time resolution ≈1 ns
- Ultra-compact active layers
- Pushing integration to the limits
- Power pulsing

ultra-heavy and compact

Comparison CLIC and LHC detector

CLIC detector:

High precision
- Jet energy resolution
→ fine-grained calorimetry
- Momentum resolution
- Impact parameter resolution

Pileup of beam-induced backgrounds
- High background rates, medium energies
- High occupancies
- Can not use vertex separation
- Need very precise timing (1 ns, 10 ns)

"No" issue of radiation damage (10^{-4} LHC)
- Except small forward calorimeters

Beam crossing "sporadic"

No trigger, read-out full 156 ns train

LHC detector:

Medium-high precision
- Very precise ECAL (CMS)
- Very precise muon tracking (ATLAS)

Pileup of minimum-bias events
- High background rates, high energies
- High occupancies
- Can use separation in Z
- Need precise time-stamping (25 ns)

Severe challenge of radiation damage

Continuous beam crossings

Trigger needed for huge data reduction

CLIC detector concepts

Based on validated ILC designs, adapted and optimised to the CLIC conditions:
- Denser HCAL in the barrel (Tungsten, 7.5 λ)
- Redesign of the vertex and forward detectors (backgrounds)
- Precise timing capabilities of most subdetectors

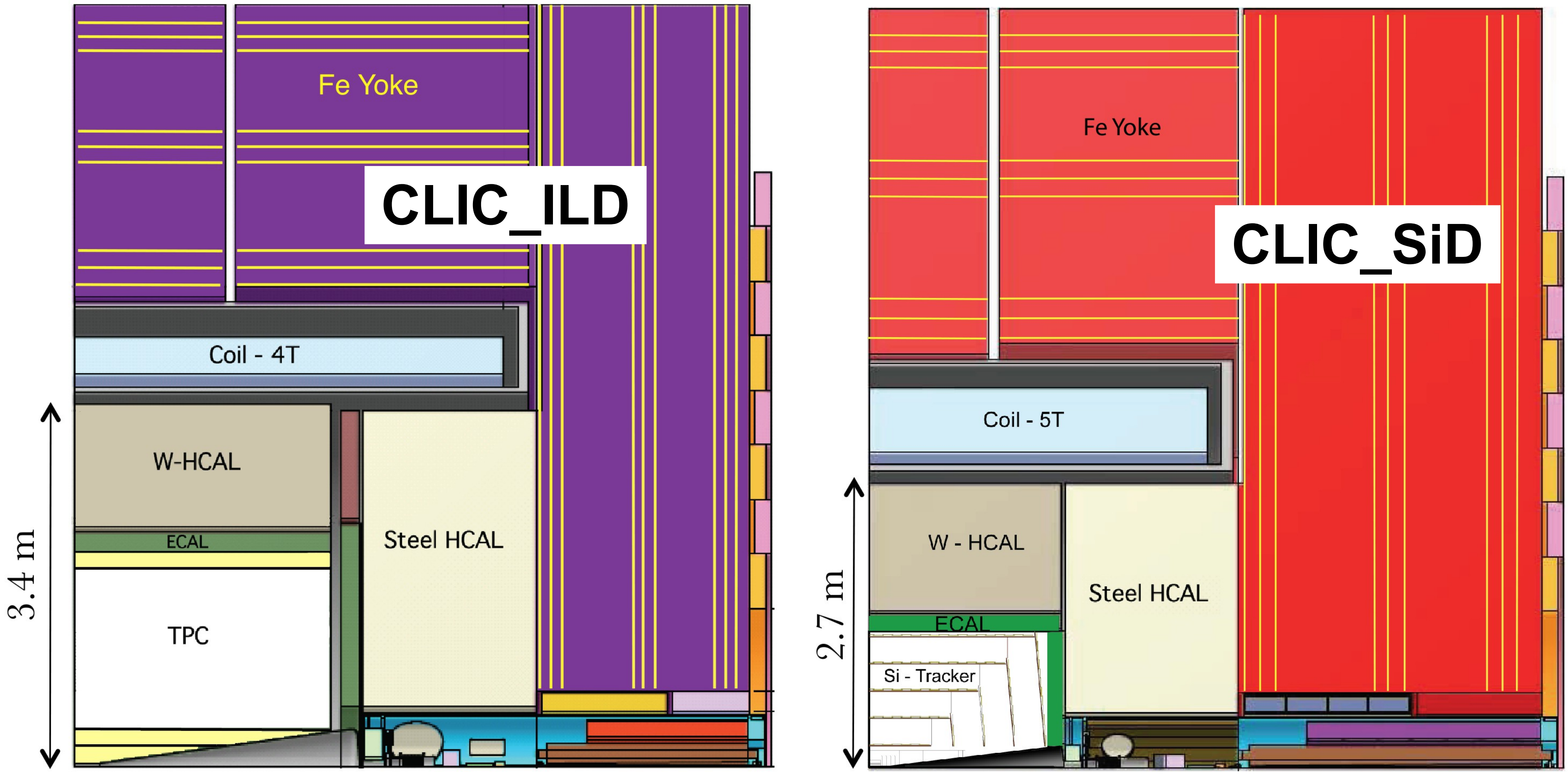

Background suppression

Triggerless readout of full bunch train:

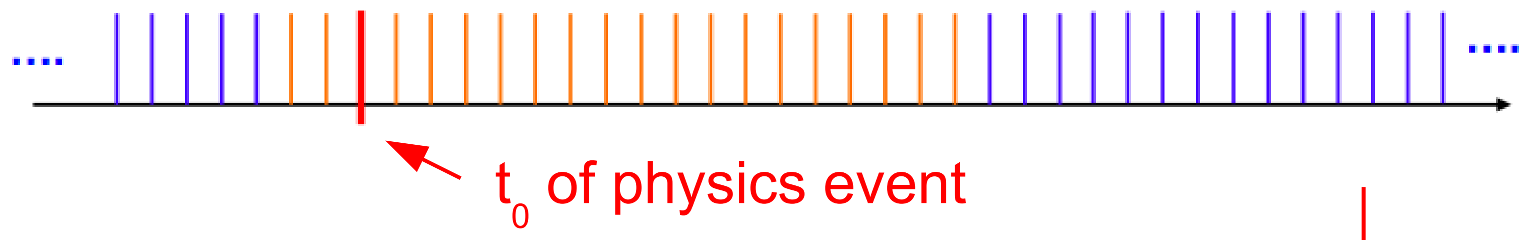

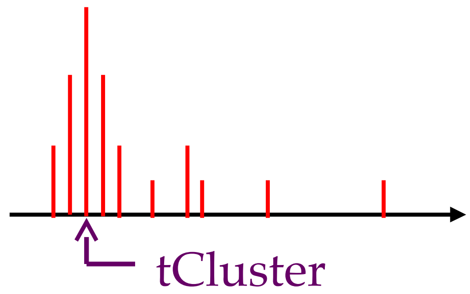

1.) **Identify t_0 of physics event in offline event filter**

- Define reconstruction window around t_0
- All hits and tracks in this window are passed to the reconstruction

→ Physics objects with precise p_T and cluster time information

2.) **Apply cluster-based timing cuts**

- Cuts depend on particle-type, p_T and detector region

→ Protects physics objects at high p_T

Time windows and hit resolutions

Used in the reconstruction software for CDR simulations:

Subdetector	Reconstruction window	hit resolution
ECAL	10 ns	1 ns
HCAL Endcaps	10 ns	1 ns
HCAL Barrel	100 ns	1 ns
Silicon Detectors	10 ns	$10/\sqrt{12}$ ns
TPC	entire bunch train	n/a

- CLIC hardware requirements
- Achievable in the calorimeters with a sampling every ≈ 25 ns

Impact of the timing cuts

$e^+e^- \to H^+H^- \to t\bar{b}b\bar{t}$ (8 jet final state)

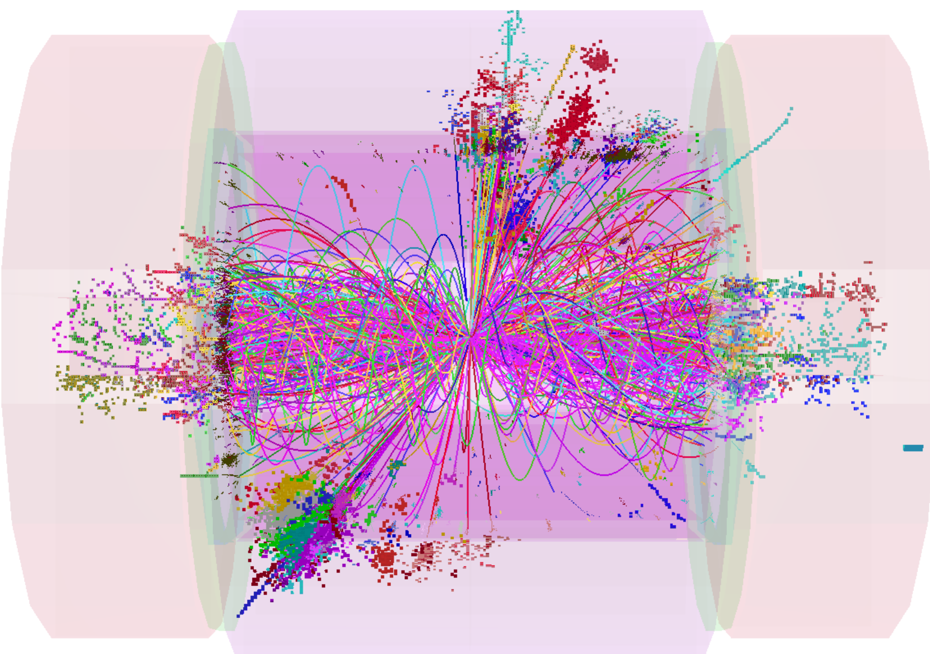

1.2 TeV background
in the reconstruction window

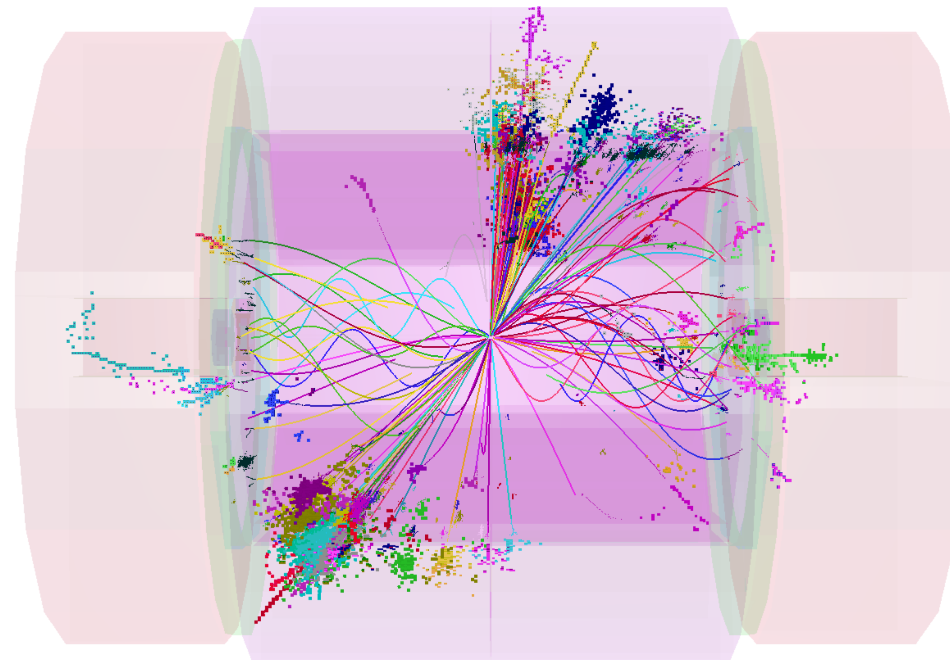

100 GeV background
after (tight) timing cuts

CLIC pixel sensor R&D

Hybrid approach:
- Thin (≈ 50 μm) sensors (e.g. Micron, CNM)
- Thinned high density ASIC in very-deep-sub-micron:
  - R&D steps: TimePix3, Smallpix
  - CLICPix
- Low-mass interconnect:
  - Micro-bump-bonding
  - Through-Silicon-Vias (R&D with CEA-Leti)
  - Chip-stitching
- Power pulsing and air cooling foreseen

Analog part of a CLICpix pixel

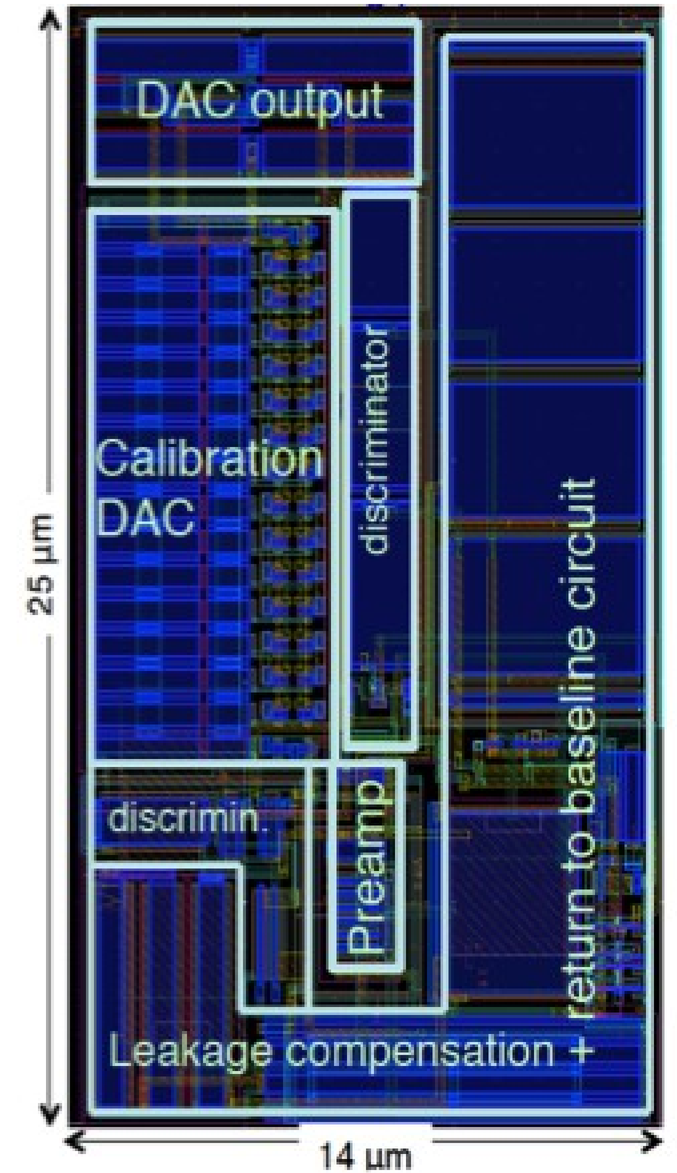

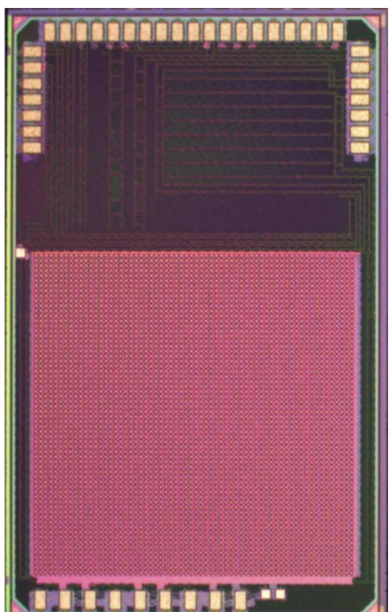

CLICpix:
- 65 nm technology
- 25 x 25 μm^2 pixels
- 4-bit TOA and TOT information (10 ns time-slicing)
- Continous power: 2 W/cm^2
- With power pulsing: 50 mW/cm^2

64 x 64 pixel demonstrator:
Chip produced by TSMC,
development of DAQ ongoing

Low-mass cooling

P ≈ 500 W in the vertex detectors

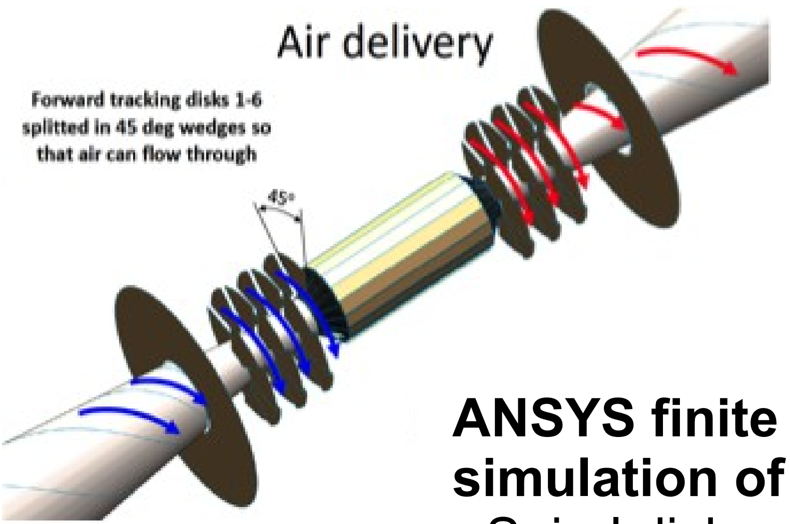

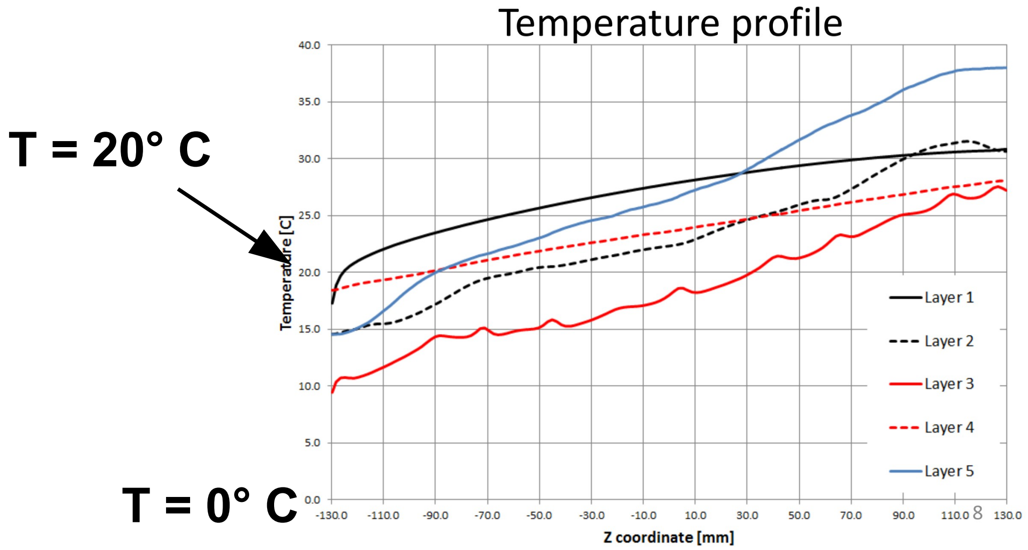

ANSYS finite element simulation of air-flow cooling:

- Spiral disk geometry
  → allows for air flow into barrel
- Sufficient heat removal
- Validation of simulation (temperature, vibrations etc.) with mock-up foreseen

vertex barrel layers

T_{in} = 0° C, m_{flow} = 20 g/s

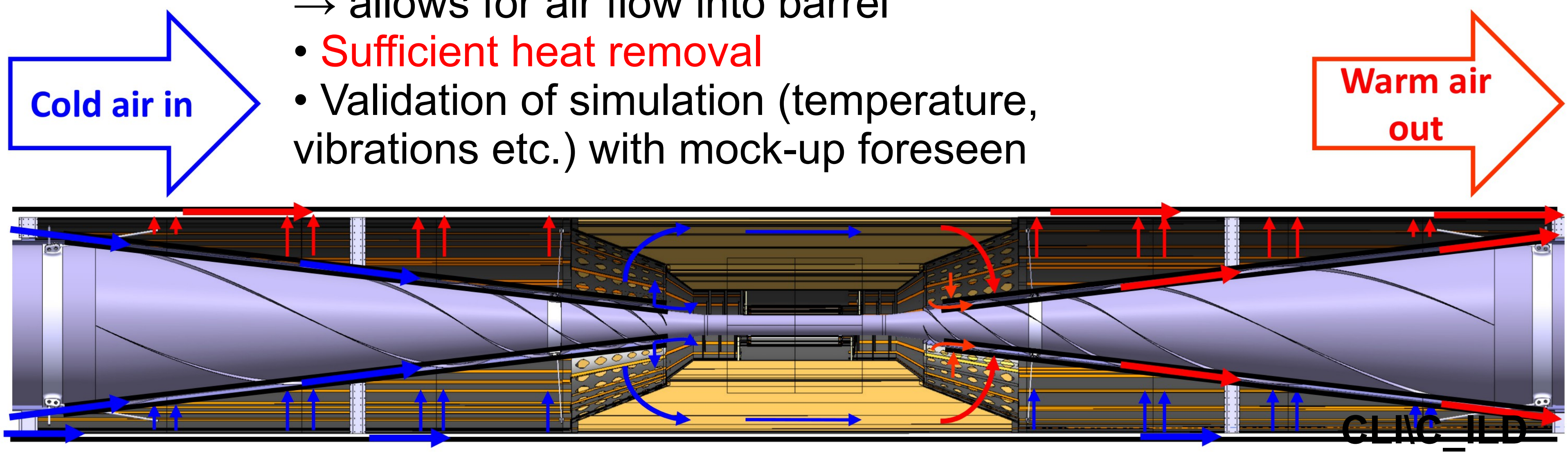

Power pulsing and delivery

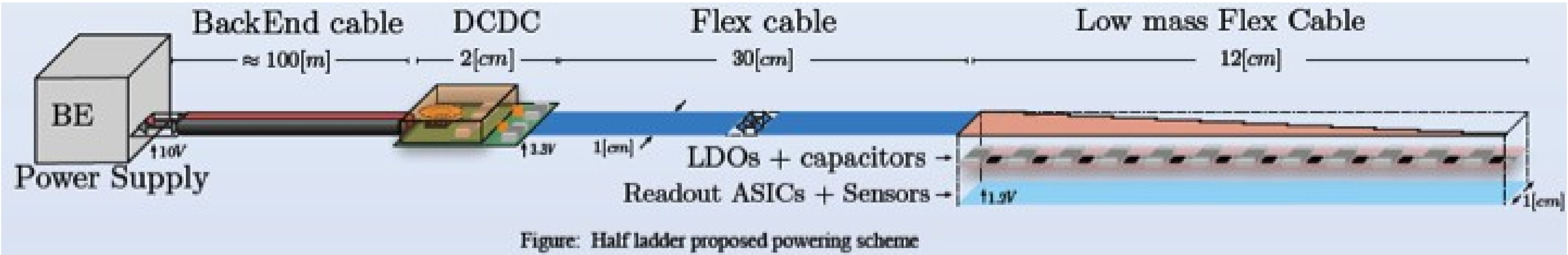

Figure: Half ladder proposed powering scheme

- CLICPix: ≈2 A at 1.2 V for 15 μs
- DC-DC converter (outside the vertex detector region)
- Flex cable
- LDOs + capacitors
- 0.07% X_0 with technology available today (Si capacitors)

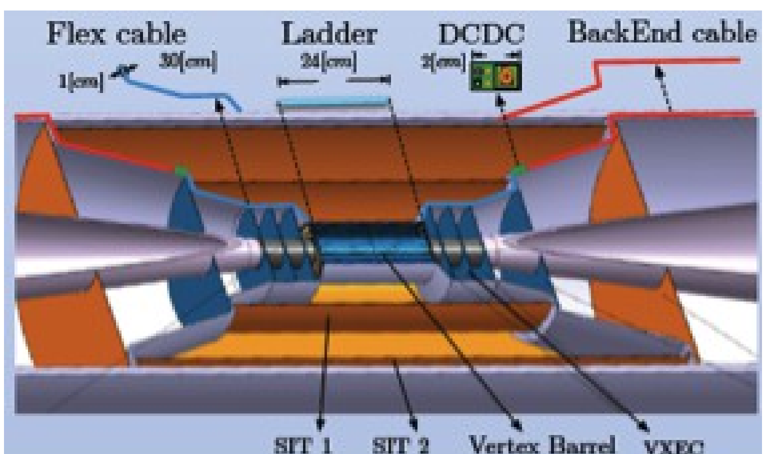

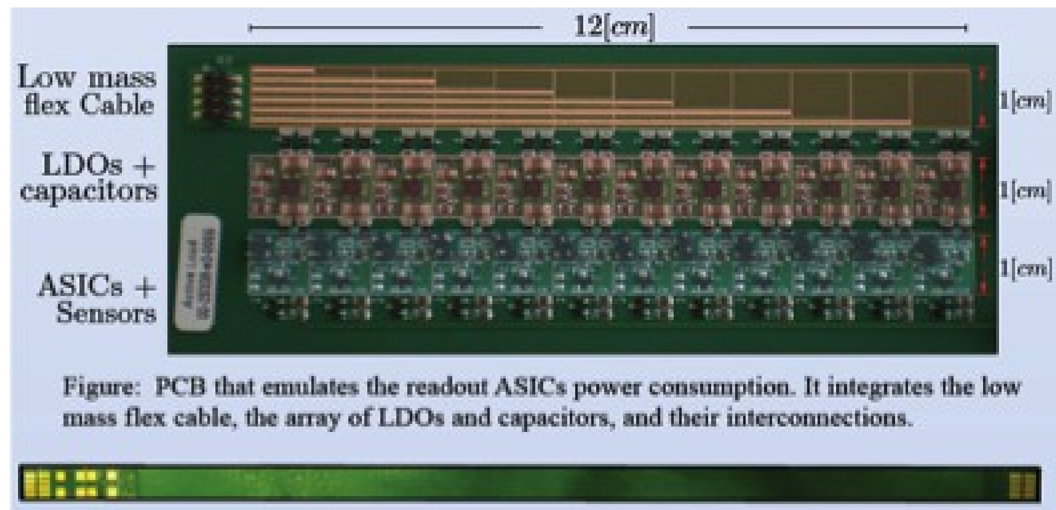

Figure: PCB that emulates the readout ASICs power consumption. It integrates the low mass flex cable, the array of LDOs and capacitors, and their interconnections.

Figure: 30 cm long Flex cable

Vertex detector geometry

Recently started to investigate the impact of the vertex detector geometry on the flavour tagging performance:

- Impact of material budget on flavour tagging performance
- Test impact of spiral geometry on physics performance
- Comparison of single layer and double layer geometry

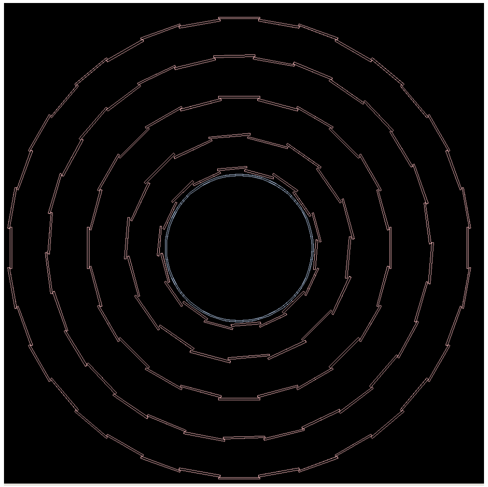

5 single layers

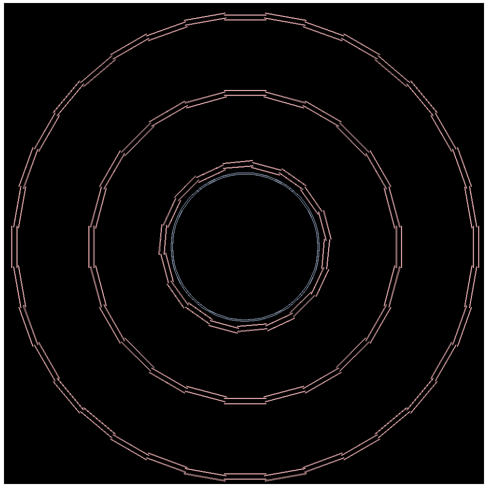

3 double layers

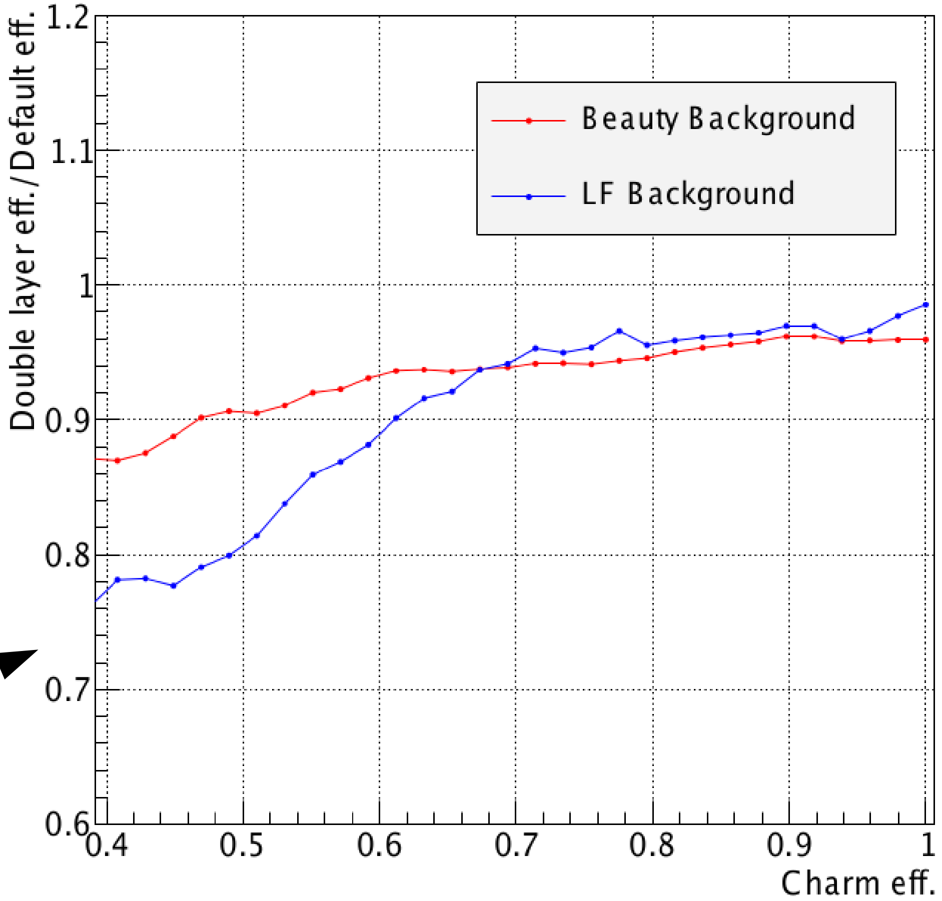

Example: Ratio of mis-identification rates for charm-tagging using 100 GeV jets

Scintillator ECAL study

Silicon surface in ECAL:
- 2600 m^2 in CLIC_ILD
- 1100 m^2 in CLIC_SiD

For comparison: CMS tracker has 200 m^2 silicon surface

→ Mayor cost driver for the detectors

New effort: Rethink ECAL design for cost optimisation
Use or combine scintillator instead of silicon readout system?

Simulation studies: Comparison of cell sizes, transverse segmentation, …

Hardware: Which minimal size the tiles is possible?

Common ILC-CLIC CALICE working group:
http://indico.cern.ch/categoryDisplay.py?categId=4379

ECAL study: first impressions

Measurements in dark room:
source with momentum
selection capability

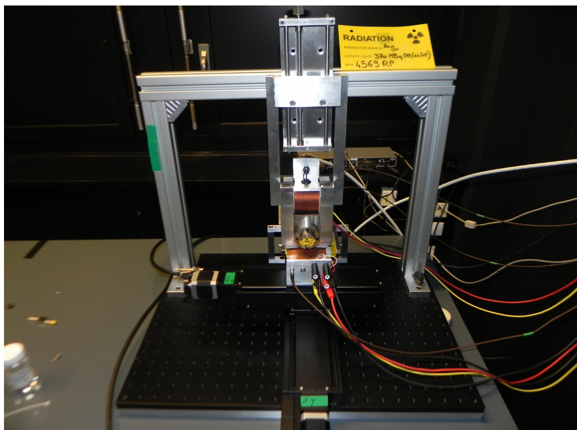

Lab at CERN

Simulation studies

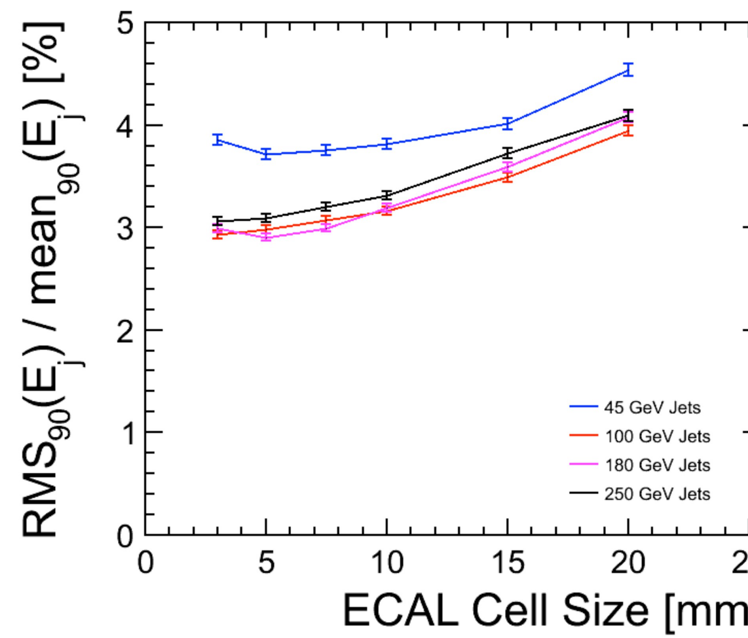

SiW ECAL, plan to repeat for ScW ECAL

Analog HCAL: scintillator/tungsten

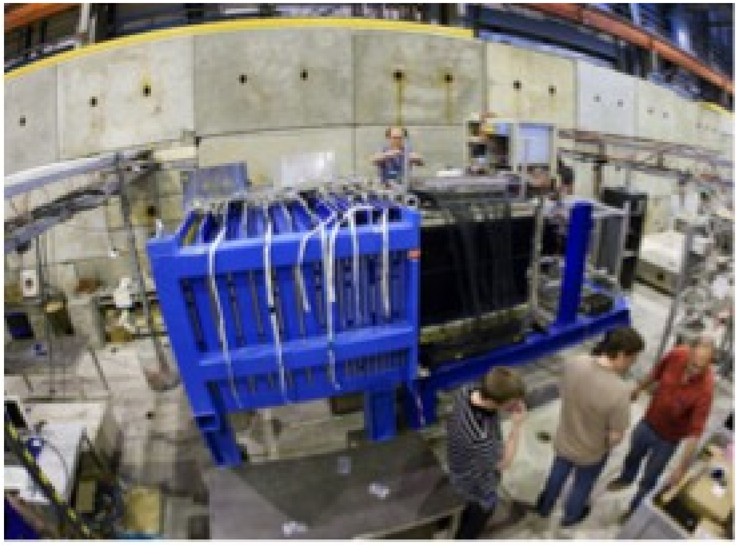

- HCAL tests with 10 mm tungsten absorber plates
- Tests in 2010 (PS) and 2011 (SPS) with scintillator active layers, 3 x 3 cm^2 cells, analog readout

→ good agreement with Geant4

long. Shower profile (π^+)

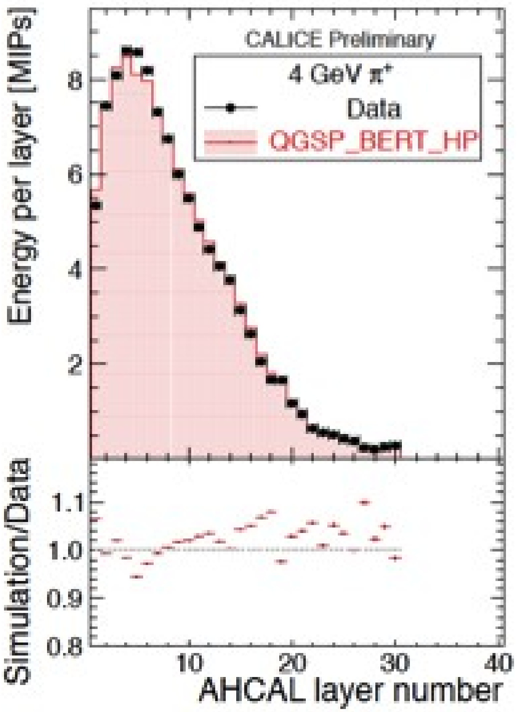

vis. energy (protons)

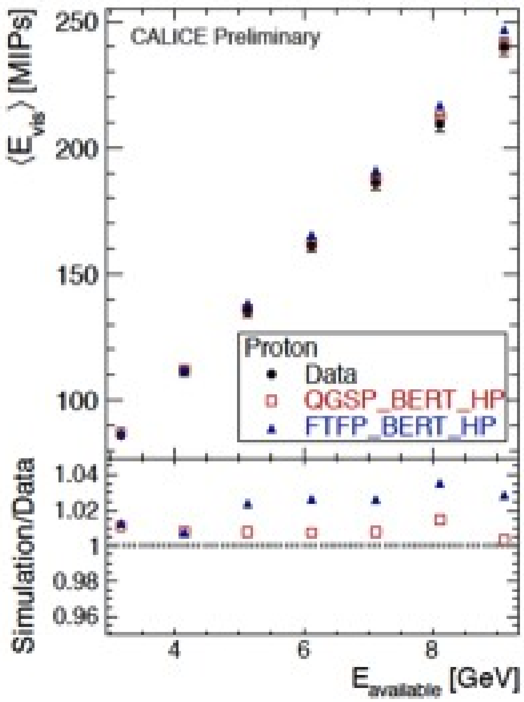

Digital HCAL: scintillator/RPC

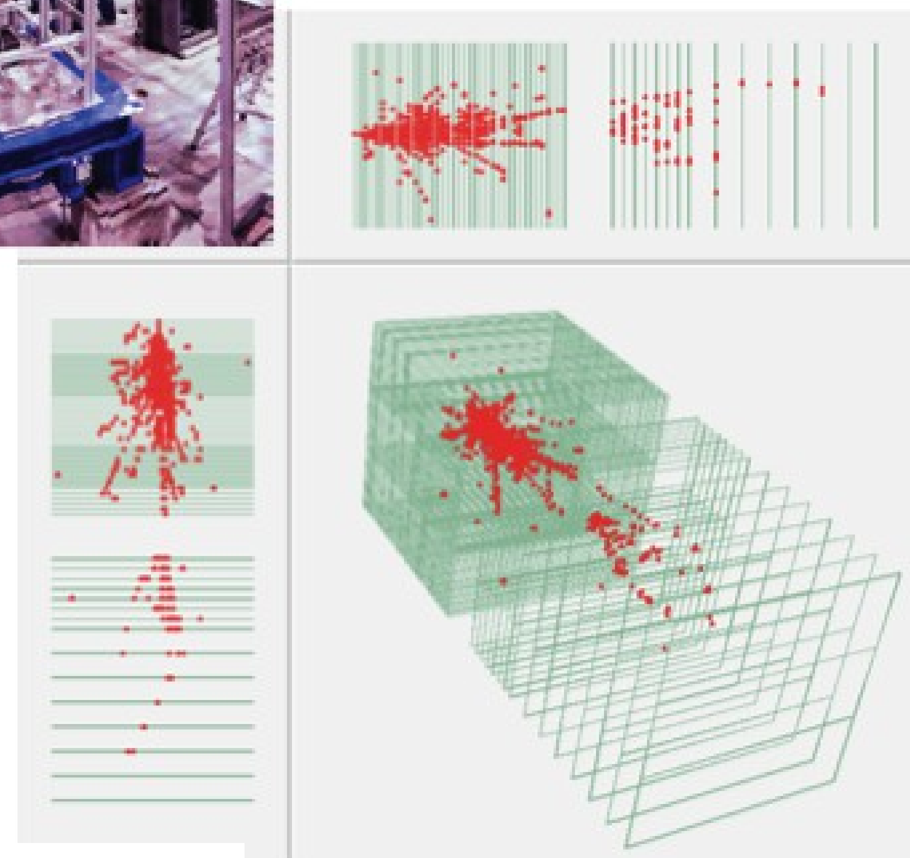

- 54 glass RPC chambers, 1 m^2 each
- Pad size 1 x 1 cm^2
- Digital readout (1 threshold), 100 ns time slicing
- Main DHCAL stack (39) and tail catcher (15)
- 500000 readout channels
- Tests in 2012 at CERN PS and SPS with tungsten absorber

Test of the di-jet mass reconstruction

Chargino and neutralino pair production:

$$e^+e^- \rightarrow \tilde{\chi}_1^+ \tilde{\chi}_1^- \rightarrow \tilde{\chi}_1^0 \tilde{\chi}_1^0 W^+W^-$$

$$e^+e^- \rightarrow \tilde{\chi}_2^0 \tilde{\chi}_2^0 \rightarrow hh\, \tilde{\chi}_1^0 \tilde{\chi}_1^0 \quad 82\%$$

$$e^+e^- \rightarrow \tilde{\chi}_2^0 \tilde{\chi}_2^0 \rightarrow Zh\, \tilde{\chi}_1^0 \tilde{\chi}_1^0 \quad 17\%$$

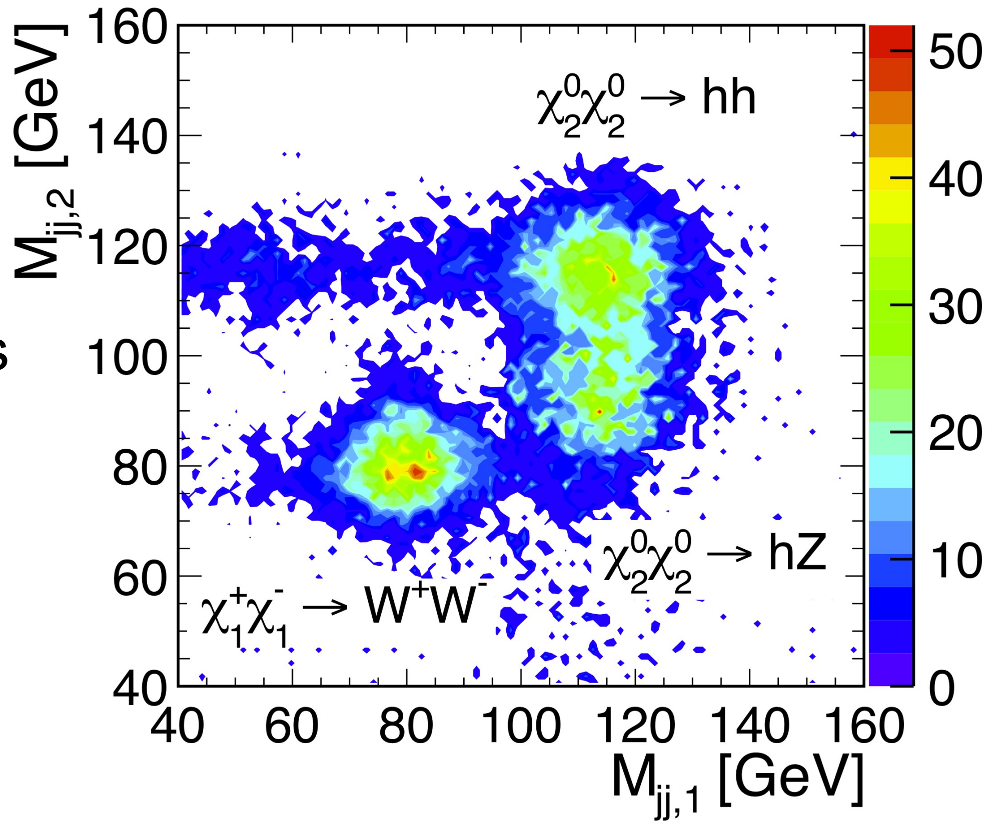

Reconstruct $W^\pm$/Z/h in hadronic decays
→ four jets and missing energy

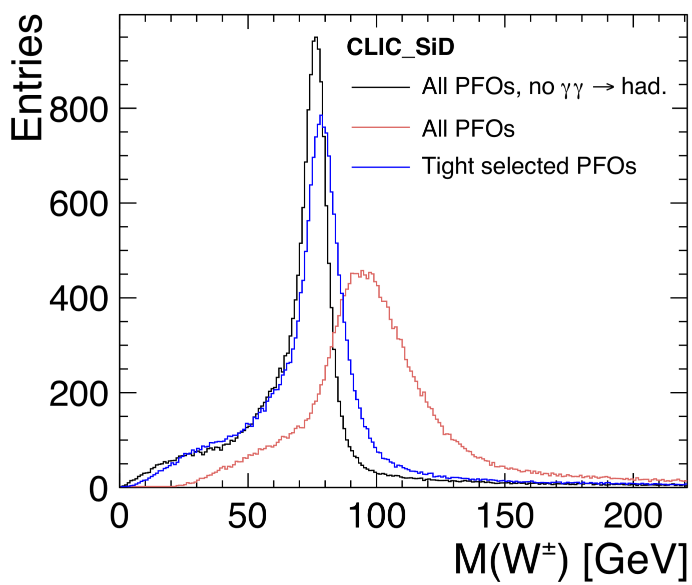

Precision on the measured gaugino masses (few hundred GeV): 1 - 1.5%

Solenoid coil

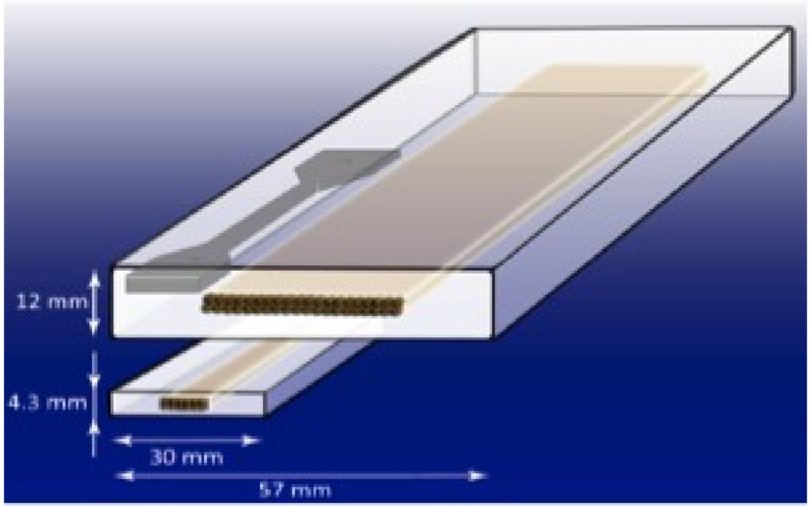

Conductor size compared to ATLAS

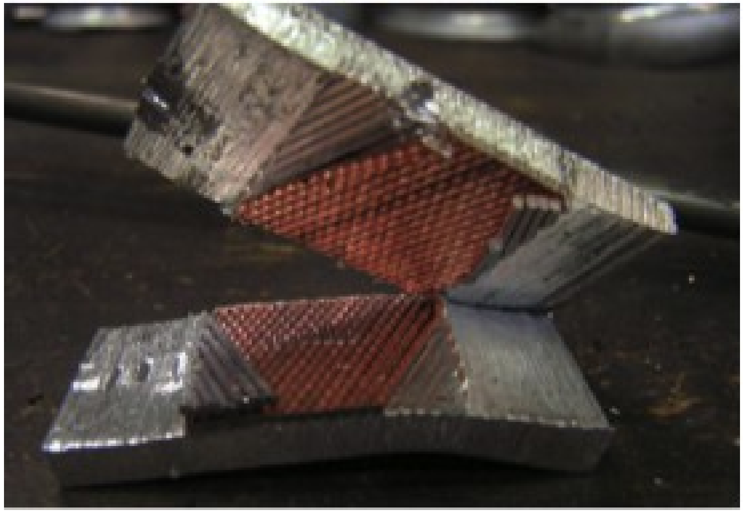

Shear test

Extrusion of Al-Ni stabilised conductor

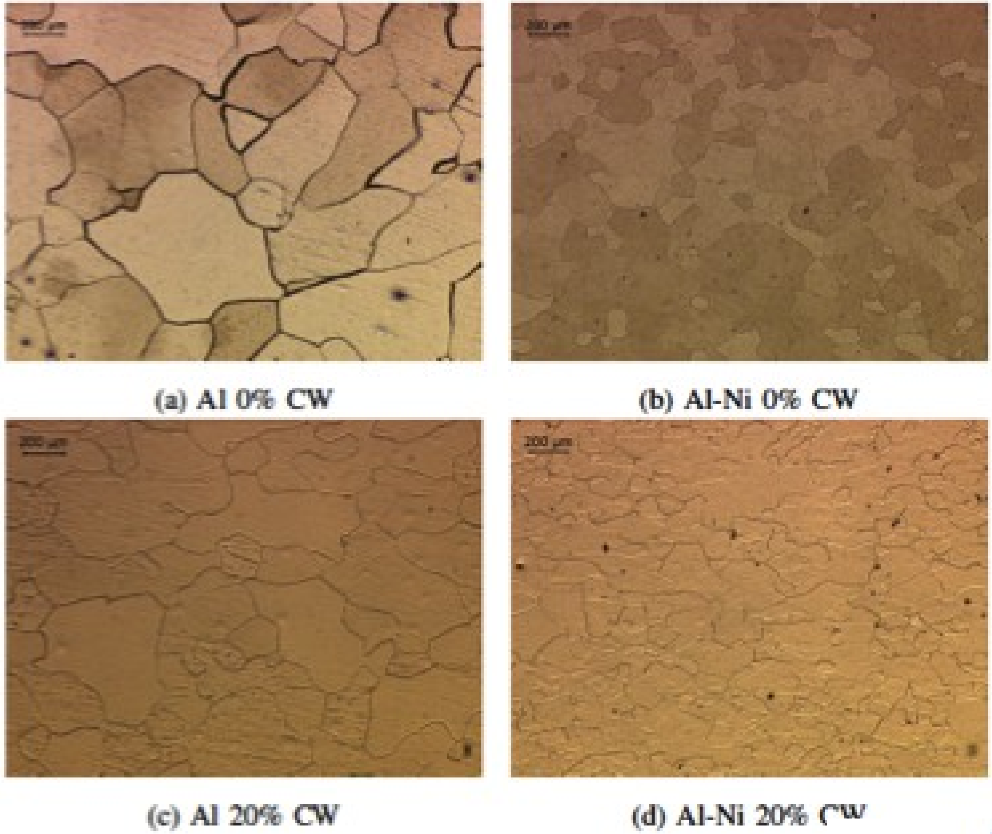

Change in material properties of Al and Al-Ni before and after cold-working

Material property tends to behave as expected

Summary and conclusions

- Physics at an CLIC e^+e^- from 350 GeV to 3 TeV can be measured with high precision, despite challenging background conditions

- Backgrounds studied in detail:
  - Require high granularity in space and time
  - Define detector requirements and guide future R&D

- The performance of the CLIC detector concepts was demonstrated using detector benchmark reactions

- **Ongoing project phase (2012-2016):**
  - CLIC detector R&D (within the international LC R&D program)
  - Further physics studies (LHC input) + detector optimisation

Backup slides

General readout considerations

3.2 γγ → hadr. interactions per bunch crossing:

- 19 TeV in the calorimeters per 156 ns bunch train
- 5000 tracks with a total momentum of 7.3 TeV

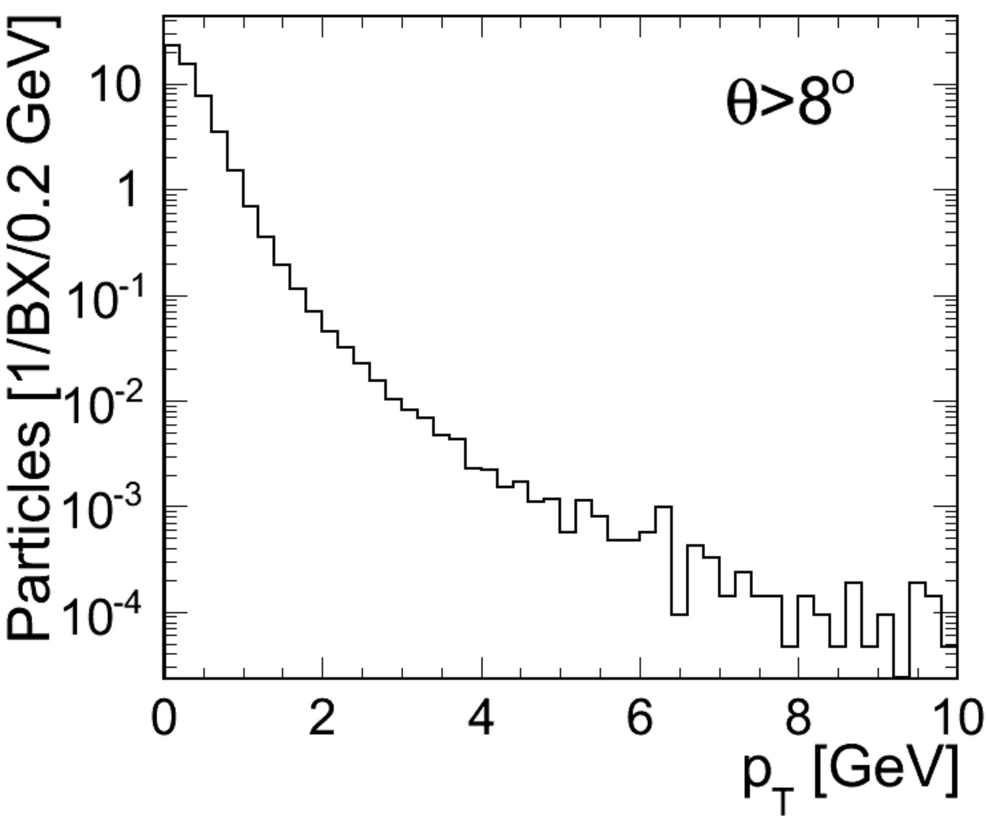

Triggerless readout of full bunch train:

- Time-stamping in tracking detectors and calorimeters
- Multi-hit storage / readout
- Filtering algorithms at reconstruction level (→ later)

Vertex detector requirements

Requirements:

- 25 x 25 μm^2 pixel size
- Material: 0.2% X_0 per layer (sensor & support):
  - Very thin materials / sensors
  - Low-power design, power pulsing, low-mass cooling
- Time stamping precision: ≈10 ns (to reject backgrounds)
- Radiation level: ≈10^{10} n_{eq} /cm^2 /yr (10^{-4} of LHC)

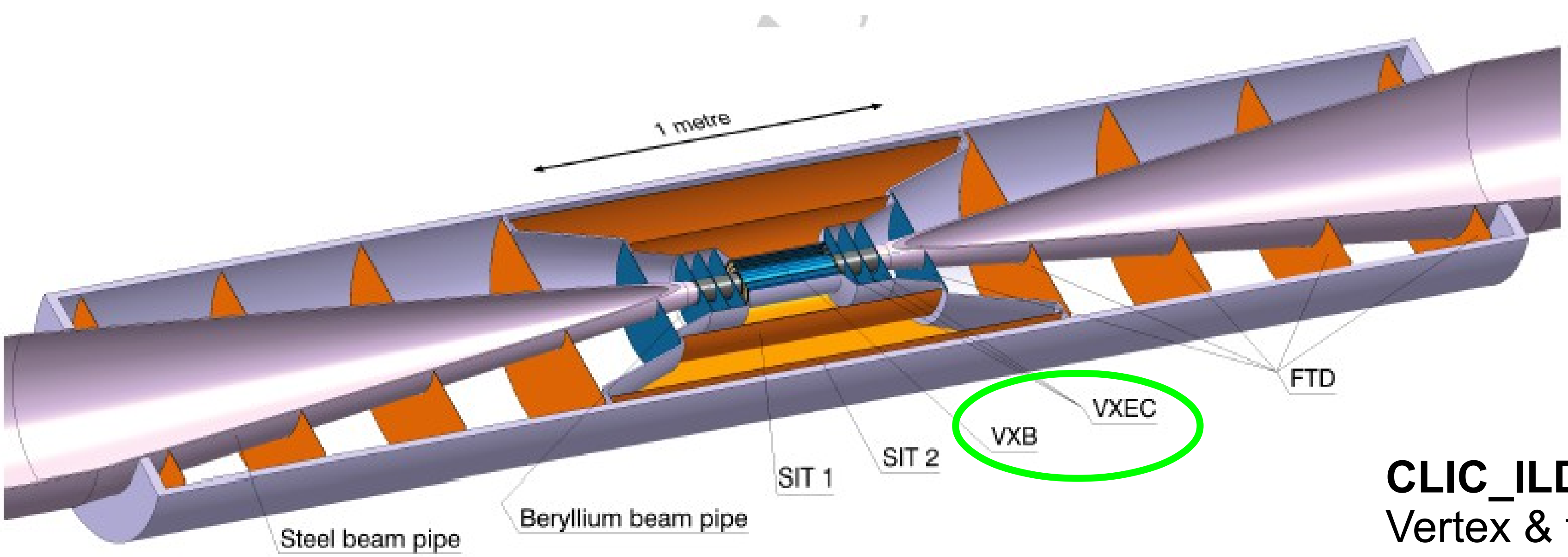

CLIC_ILD:
Vertex & forward tracking

Vertex detector backgrounds

Incoherent pair background determines:
Locations of vertex detector & forward tracking disks, design of beam pipe

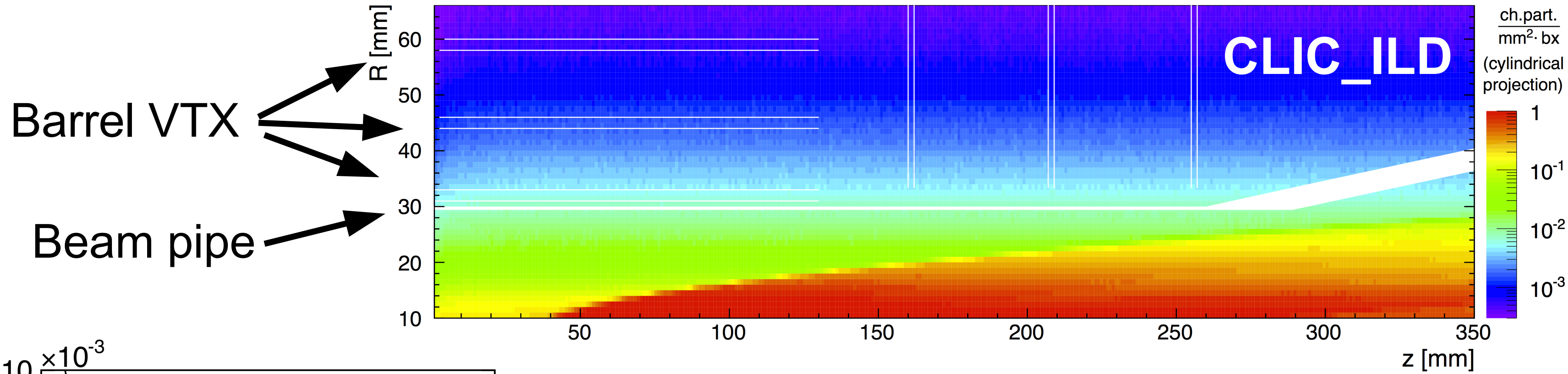

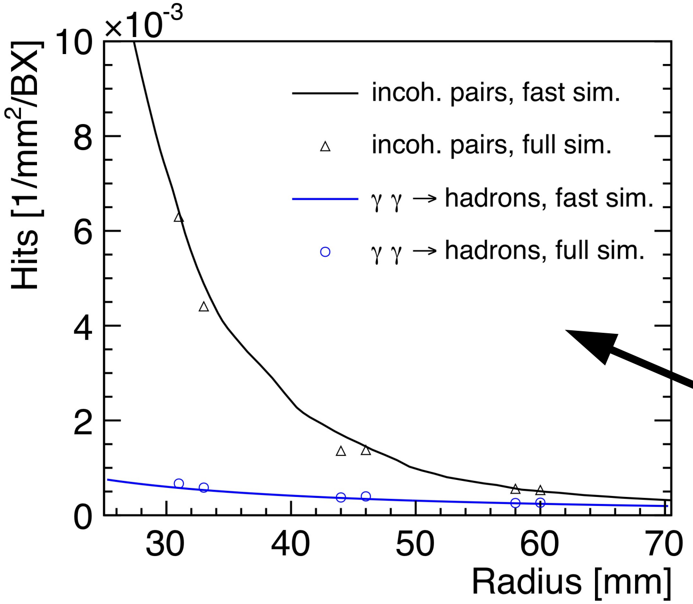

- Pair background mostly at low radii
- Inner radius of barrel vertex detector: 31 mm (CLIC_ILD), 27 mm (CLIC_SiD)
- Barrel: up to 1.9% train occupancy / pixel
- Forward: up to 2.9% train occupancy / pixel

(including safety factors of 5)

Vertex detector layouts

CLIC_ILD: 3 double layers, 1.84 · 10^9 pixels

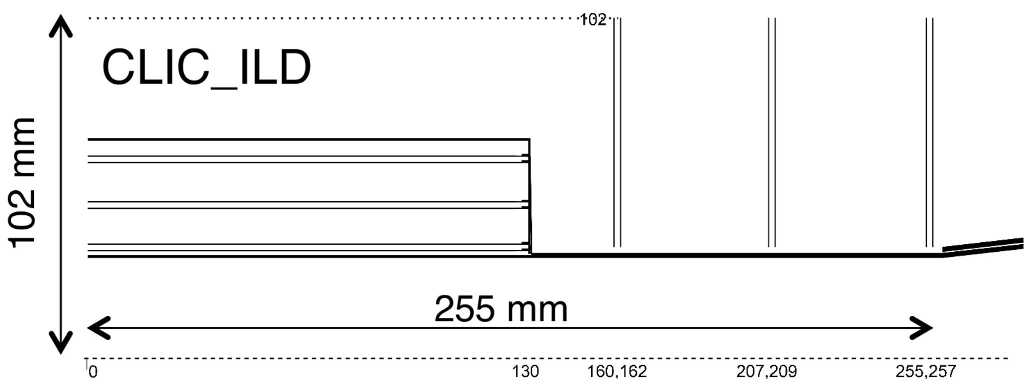

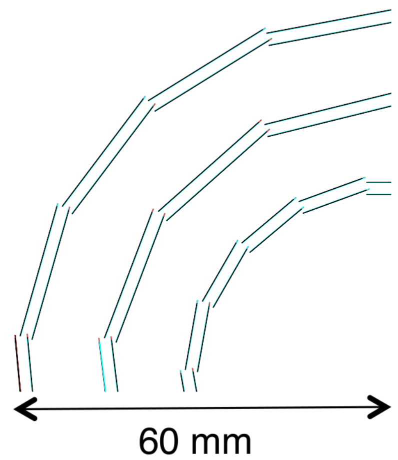

CLIC_SiD: 5 single layers, 2.76 · 10^9 pixels

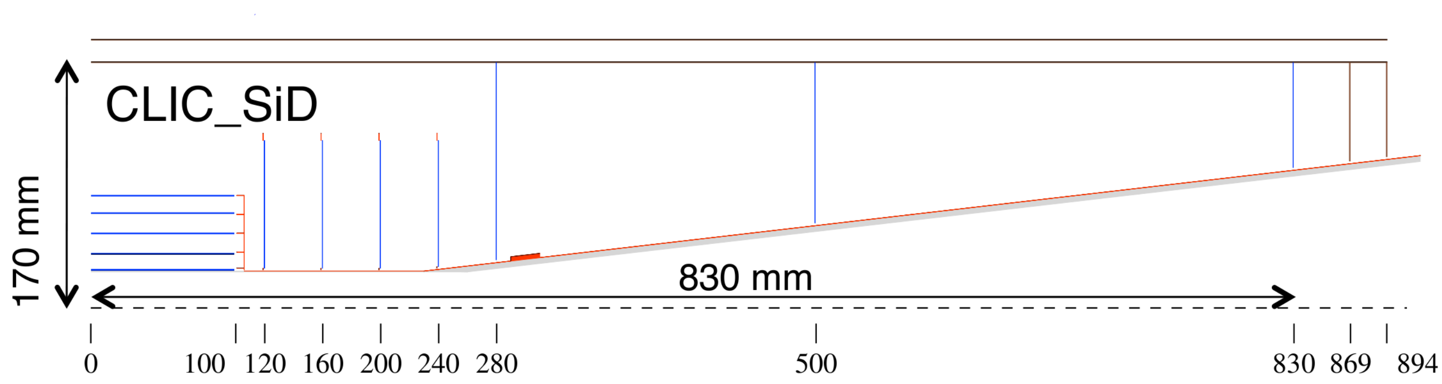

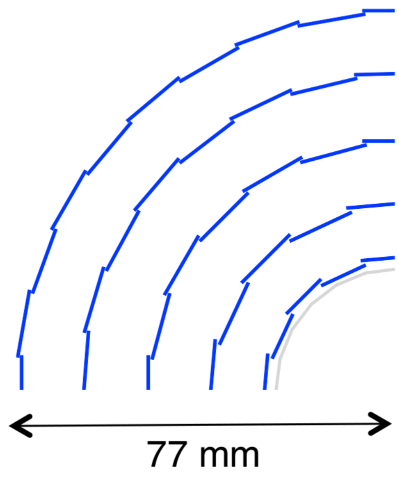

Tracking in CLIC_ILD

TPC + silicon tracking in 4T field

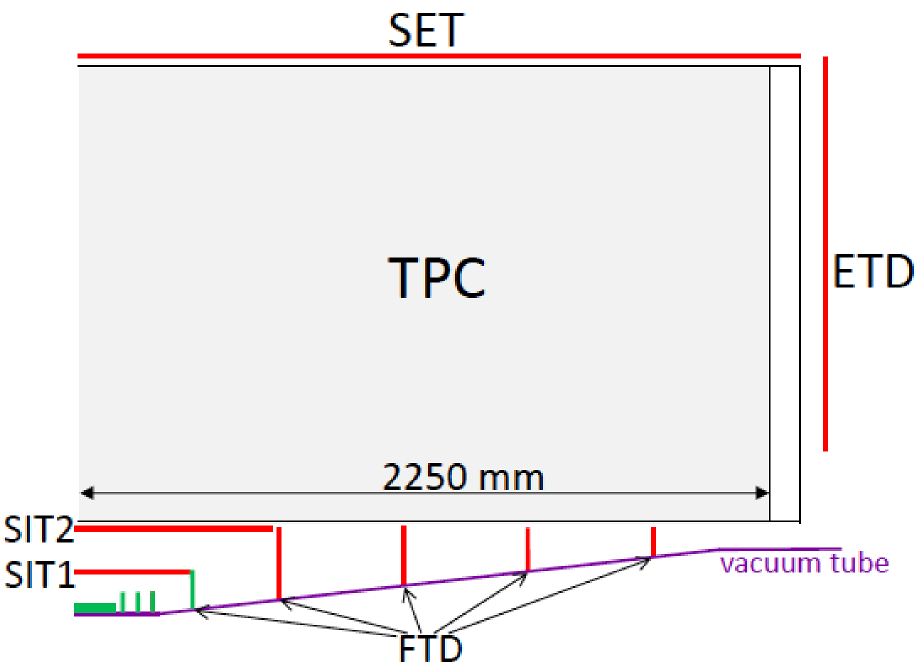

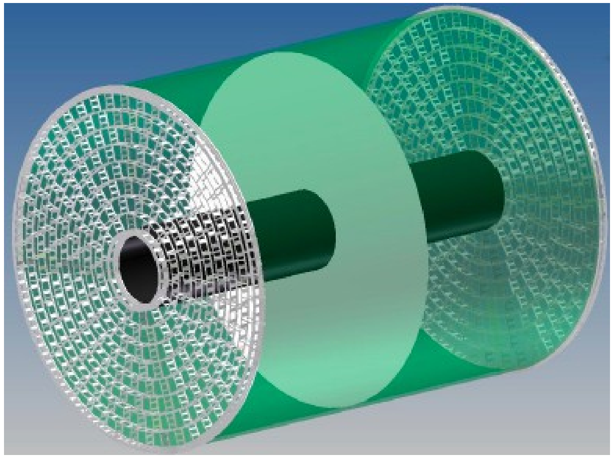

Time projection chamber (TPC)

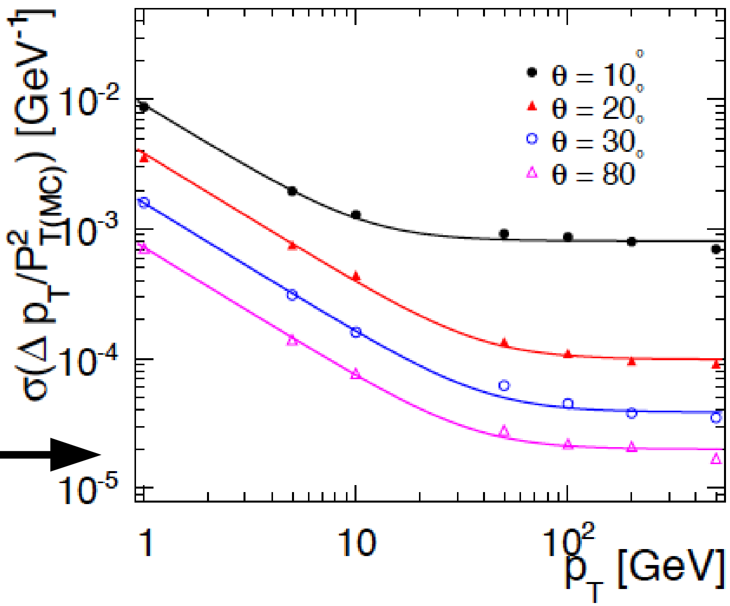

Performance goal on momentum resolution achieved

Occupancies in the TPC

The readout time of the TPC is much longer than a CLIC bunch train
→ The TPC integrates the background of a full train at CLIC

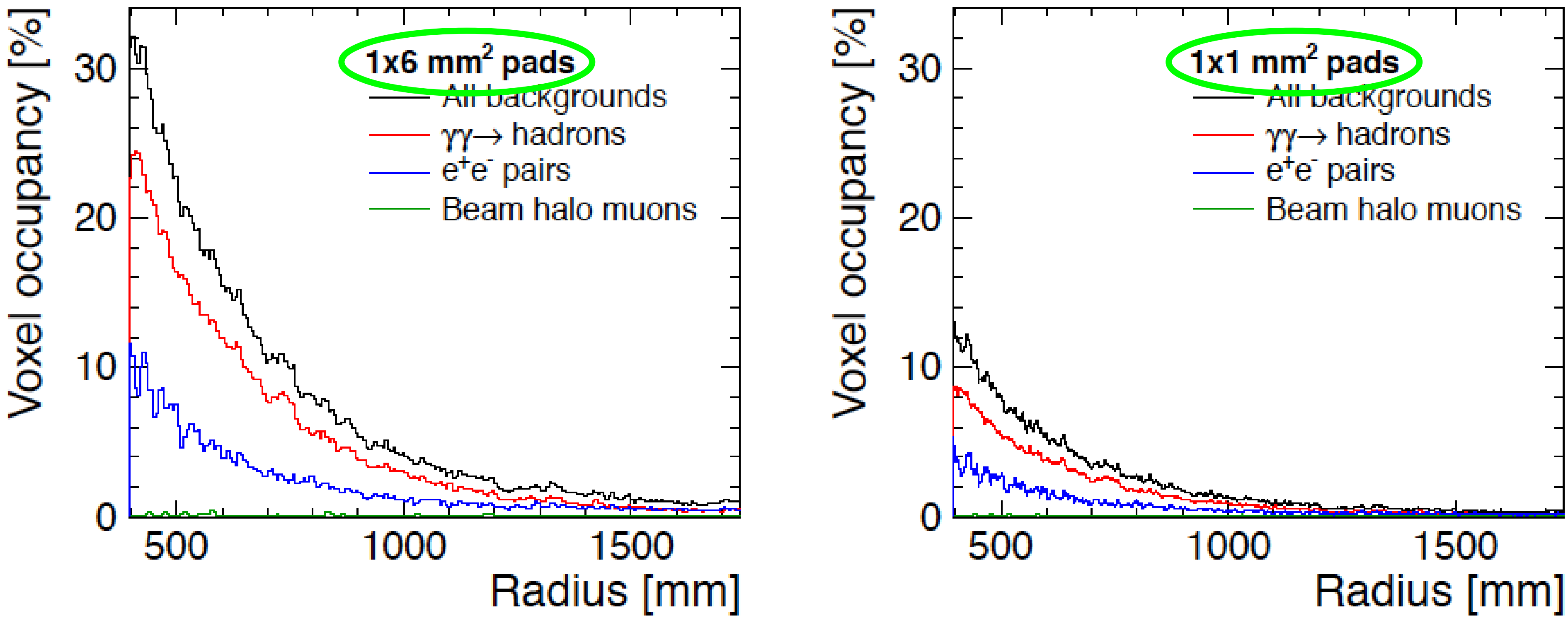

Plots are for Gas Electron Multiplier (GEM) + Pad readout, voxels of 25 ns

→ A TPC at CLIC may need a larger inner radius or very small pads
Similar study with micromegas + pixel readout is starting

Tracking in CLIC_SiD

All silicon tracker in 5T field:
- Vertex detector and tracker viewed as one system
- Combined seeding and tracking

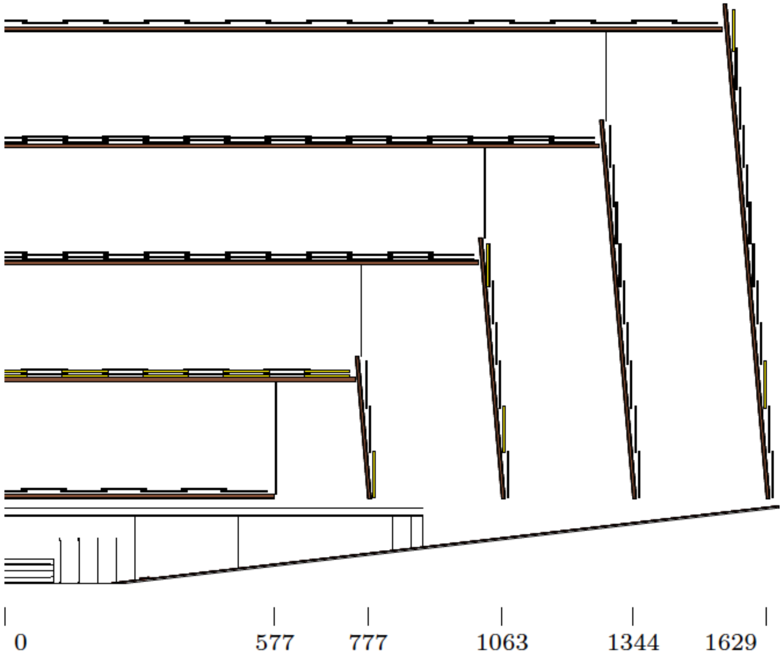

Two readout (KPiX) chips bump bonded to the sensor

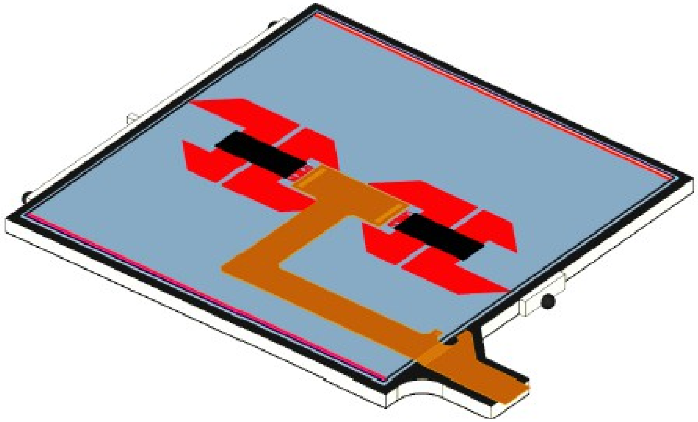

Performance goal on momentum resolution achieved

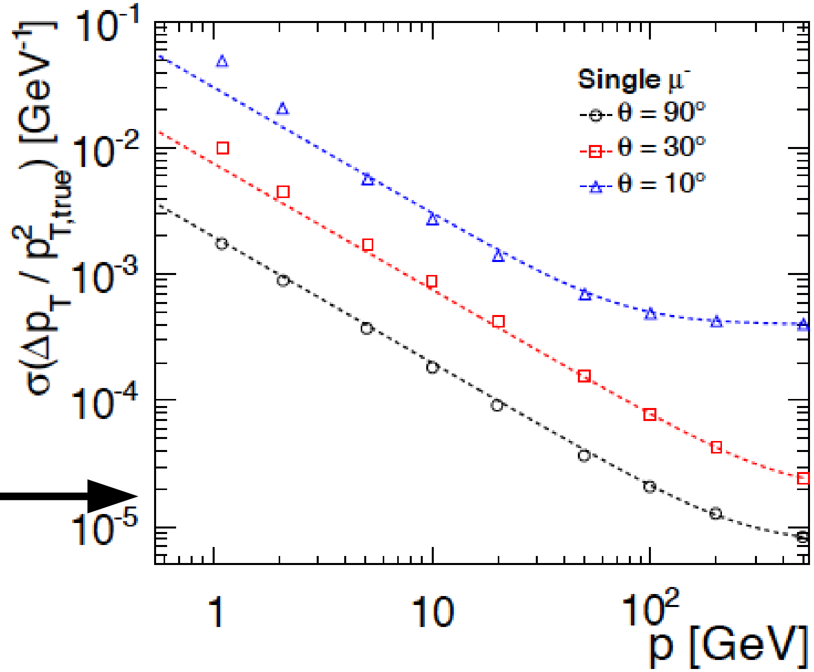

HCAL resolution

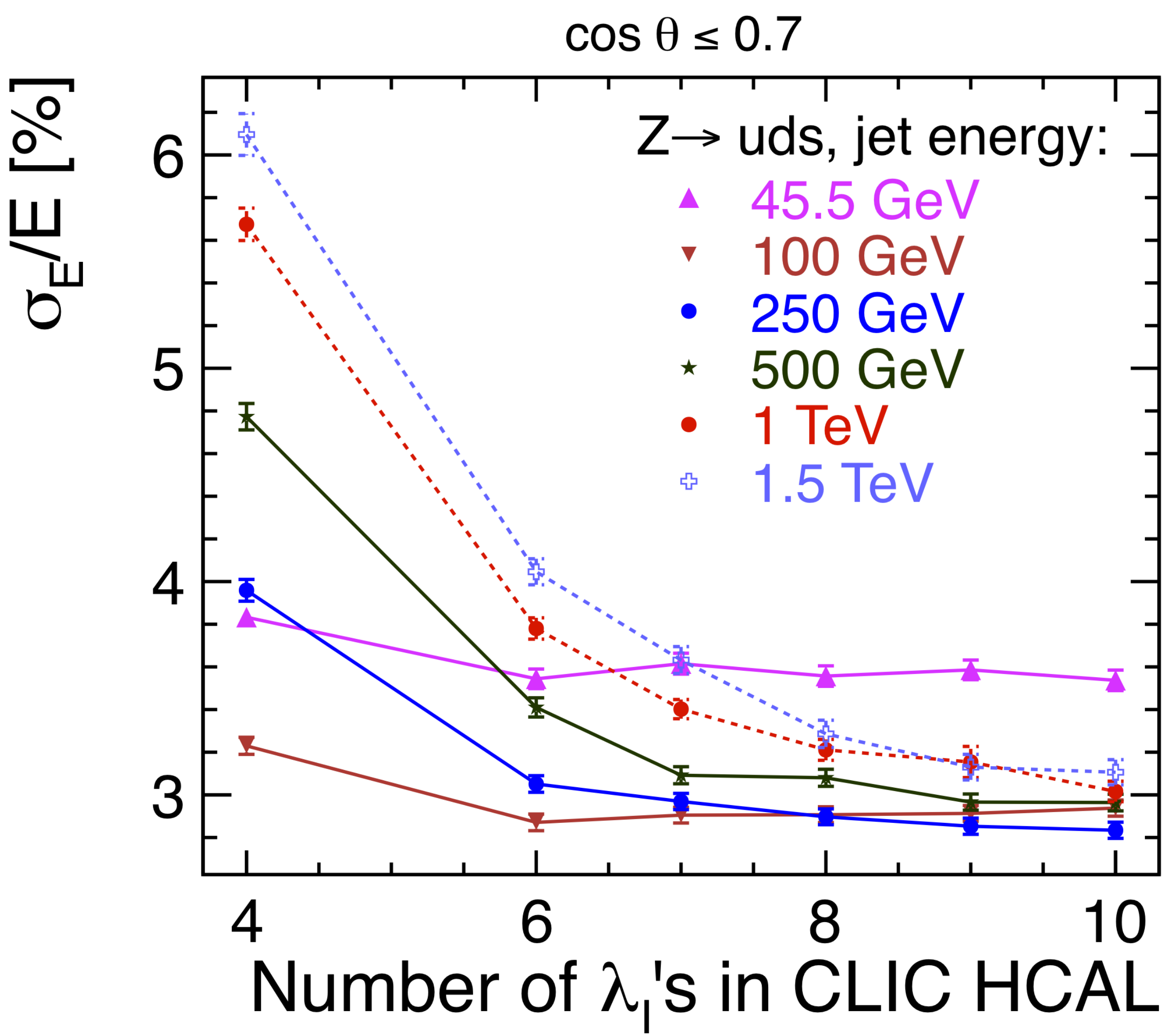

Calorimetry: technology

ECAL:

- Silicon pads or scintillator
- Tungsten absorber
- Cell sizes: 25 mm^2 (CLIC_ILD)
  13 mm^2 (CLIC_SiD)
- 30 layers in depth
- 23 X_0 and 1 λ

HCAL:

- Several options for sensors
- Tungsten (barrel), steel (forward)
- Cell sizes: 9 cm^2 (analog)
  1 cm^2 (digital)
- 60 - 75 layers in depth
- 7.5 λ

SiD ECAL

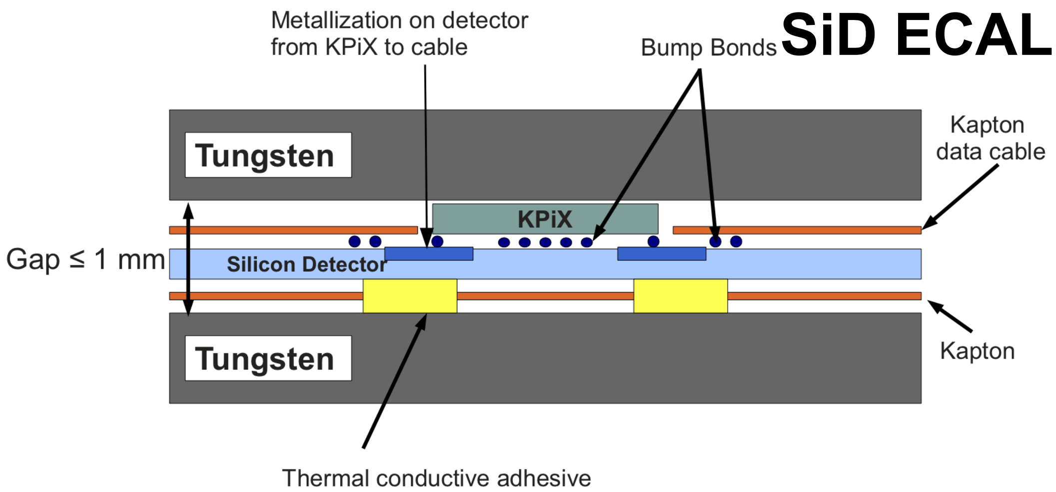

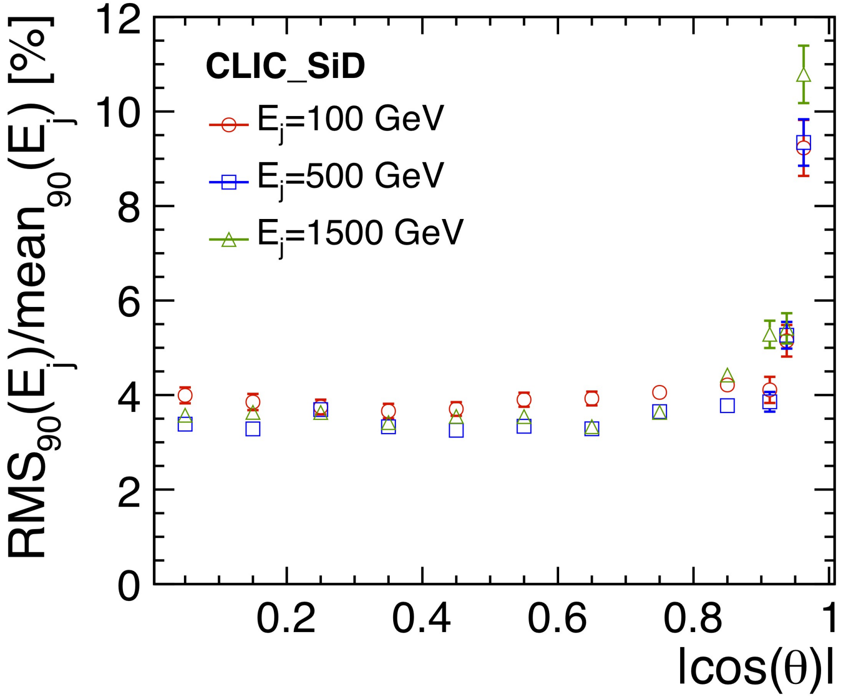

Time development in hadronic showers

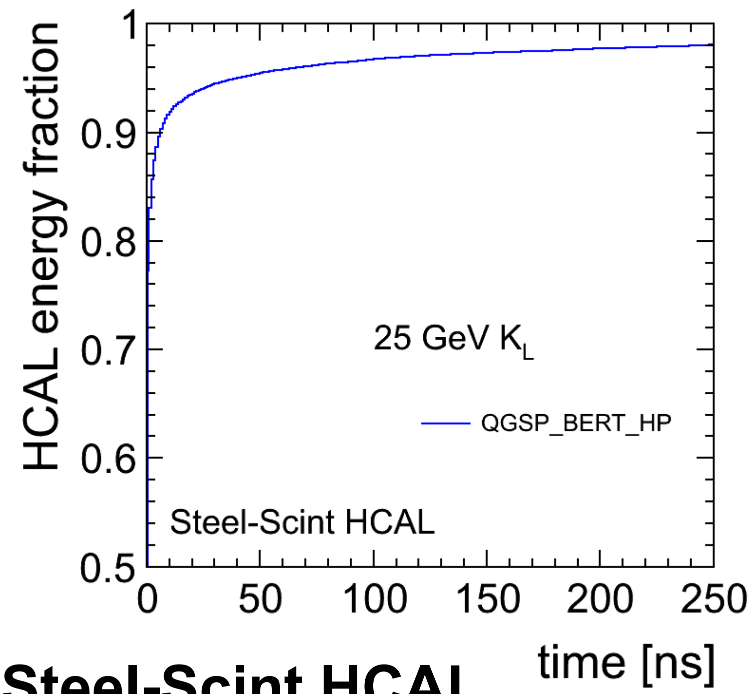

Steel-Scint HCAL

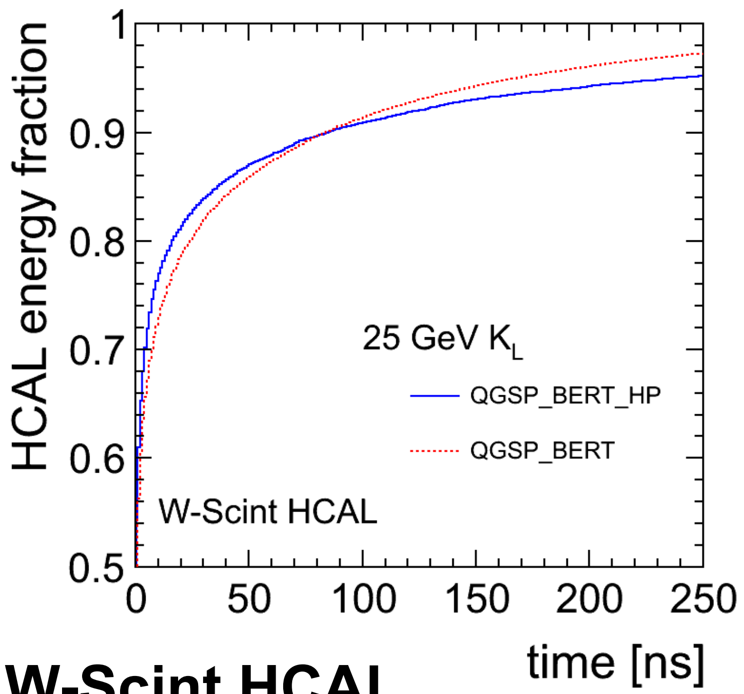

W-Scint HCAL

- In steel 90% of the energy is recorded within 6 ns (corrected for time-of-flight)
- In tungsten only 82% of the energy is deposited within 25 ns:

(much larger component of the energy in nuclear fragments)

→ Energy resolution degrades if not the majority of calorimeter hits is read

→ Need to integrate over ≈100 ns in the reconstruction, keeping the background level low

Software compensation

High granularity of the calorimeter can be used to distinguish between electromagnetic (dense) and hadronic (less dense) shower components

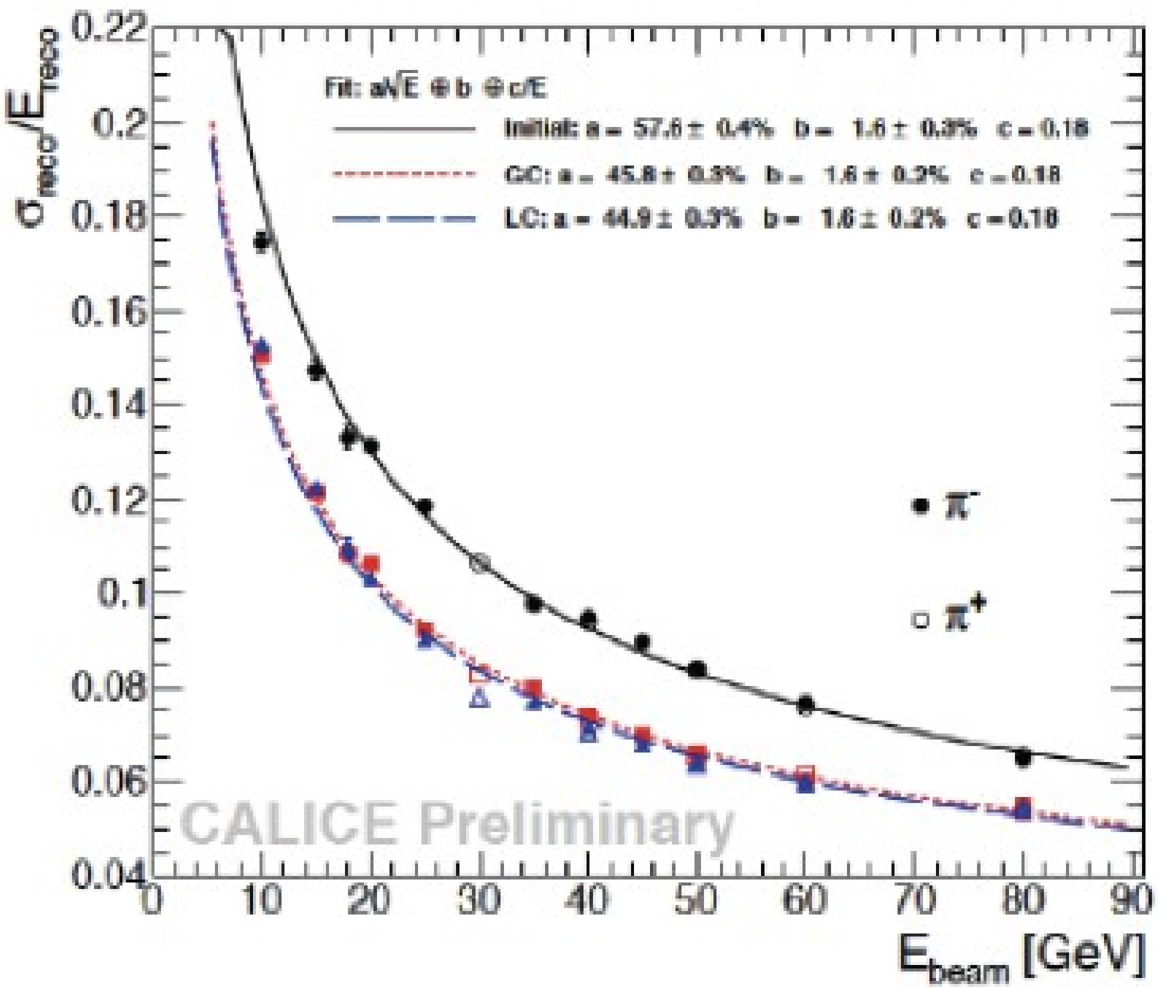

CALICE
Steel-AHCAL data

Improved resolution (20% better) and linearity

PFO based timing cuts

Region	p_t *range*	Time cut
Photons		
central ($\cos\theta \leq 0.975$)	$0.75\ \text{GeV} \leq p_t < 4.0\ \text{GeV}$ $0\ \text{GeV} \leq p_t < 0.75\ \text{GeV}$	$t < 2.0$ nsec $t < 1.0$ nsec
forward ($\cos\theta > 0.975$)	$0.75\ \text{GeV} \leq p_t < 4.0\ \text{GeV}$ $0\ \text{GeV} \leq p_t < 0.75\ \text{GeV}$	$t < 2.0$ nsec $t < 1.0$ nsec
Neutral hadrons		
central ($\cos\theta \leq 0.975$)	$0.75\ \text{GeV} \leq p_t < 8.0\ \text{GeV}$ $0\ \text{GeV} \leq p_t < 0.75\ \text{GeV}$	$t < 2.5$ nsec $t < 1.5$ nsec
forward ($\cos\theta > 0.975$)	$0.75\ \text{GeV} \leq p_t < 8.0\ \text{GeV}$ $0\ \text{GeV} \leq p_t < 0.75\ \text{GeV}$	$t < 2.0$ nsec $t < 1.0$ nsec
Charged PFOs		
all	$0.75\ \text{GeV} \leq p_t < 4.0\ \text{GeV}$ $0\ \text{GeV} \leq p_t < 0.75\ \text{GeV}$	$t < 3.0$ nsec $t < 1.5$ nsec

- Track-only minimum p_t: 0.5 GeV
- Track-only maximum time at ECAL: 10 nsec

Influence of pileup

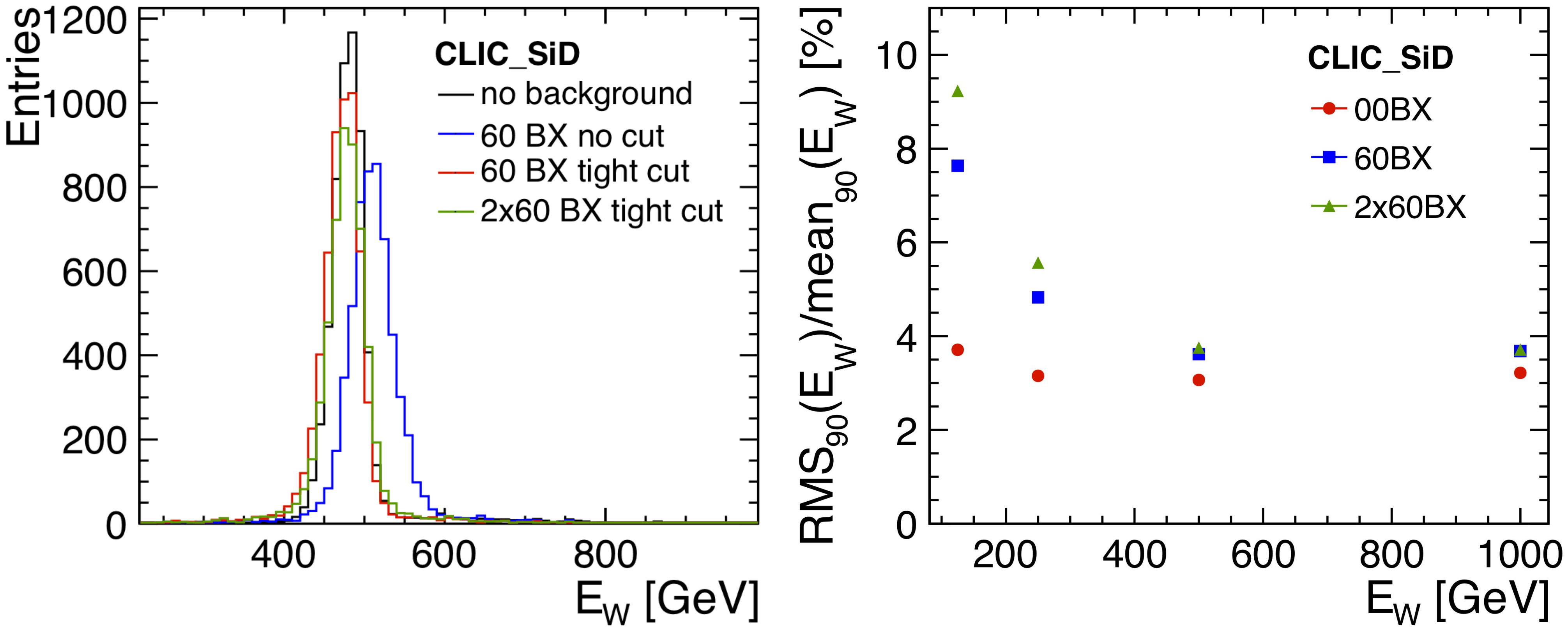

Jet reconstruction at CLIC I

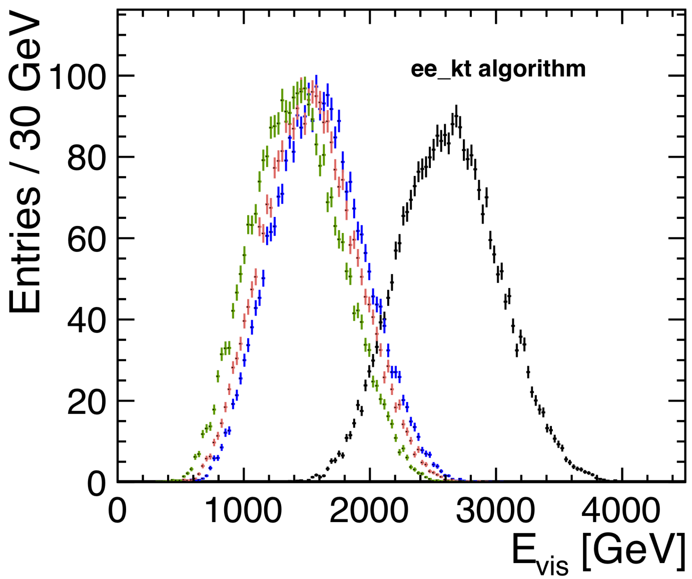

$$e^+e^- \rightarrow \tilde{q}_R\tilde{q}_R \rightarrow q\bar{q}\,\tilde{\chi}_1^0\,\tilde{\chi}_1^0$$

Two jets + missing energy

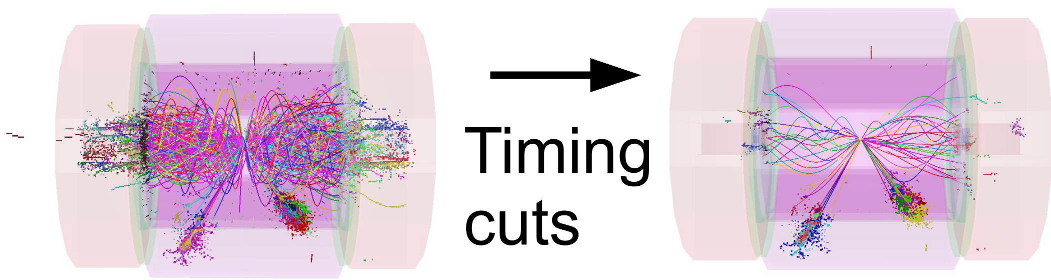

- Using Durham k_T à la LEP

→ Timing cuts are effective, but not sufficient

Jet reconstruction at CLIC II

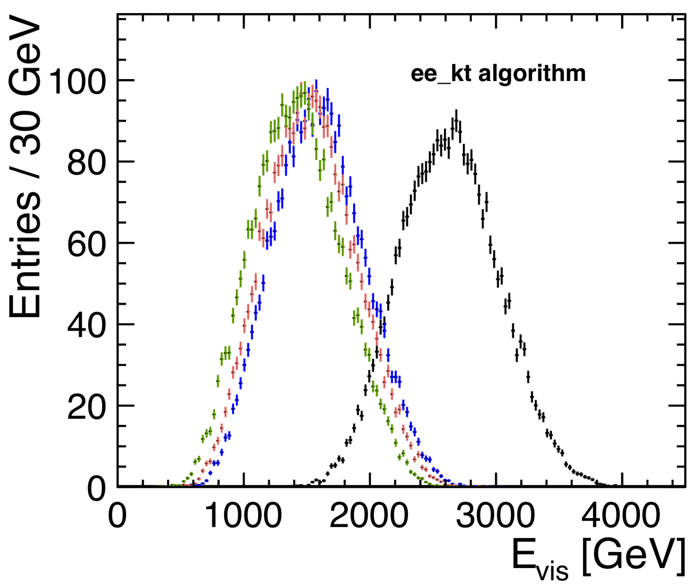

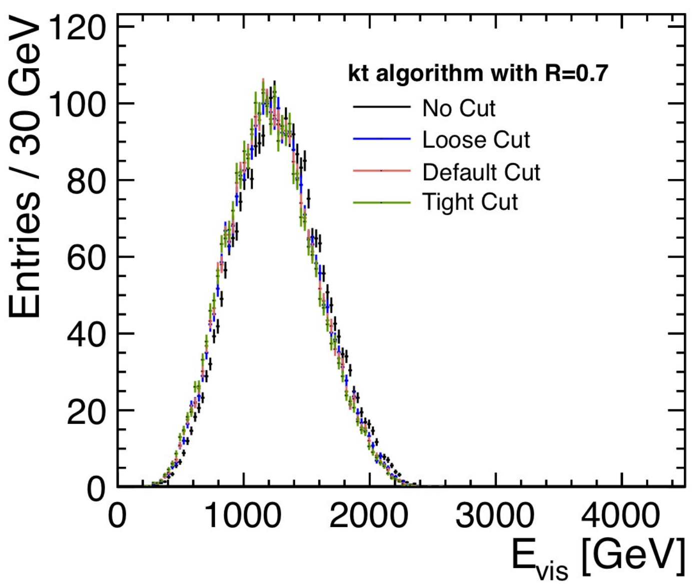

$$e^+e^- \to \tilde{q}_R\tilde{q}_R \to q\bar{q}\,\tilde{\chi}_1^0\,\tilde{\chi}_1^0$$

Two jets + missing energy

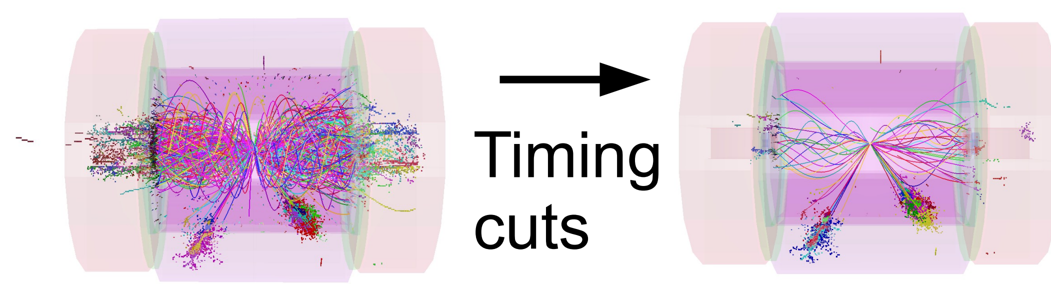

- Using Durham k_T à la LEP

→ Timing cuts are effective, but not sufficient

- “hadron collider” k_T, R = 0.7

→ Background significantly reduced further

→ Need timing cut + jet finding for background reduction

W^+W^- and ZZ

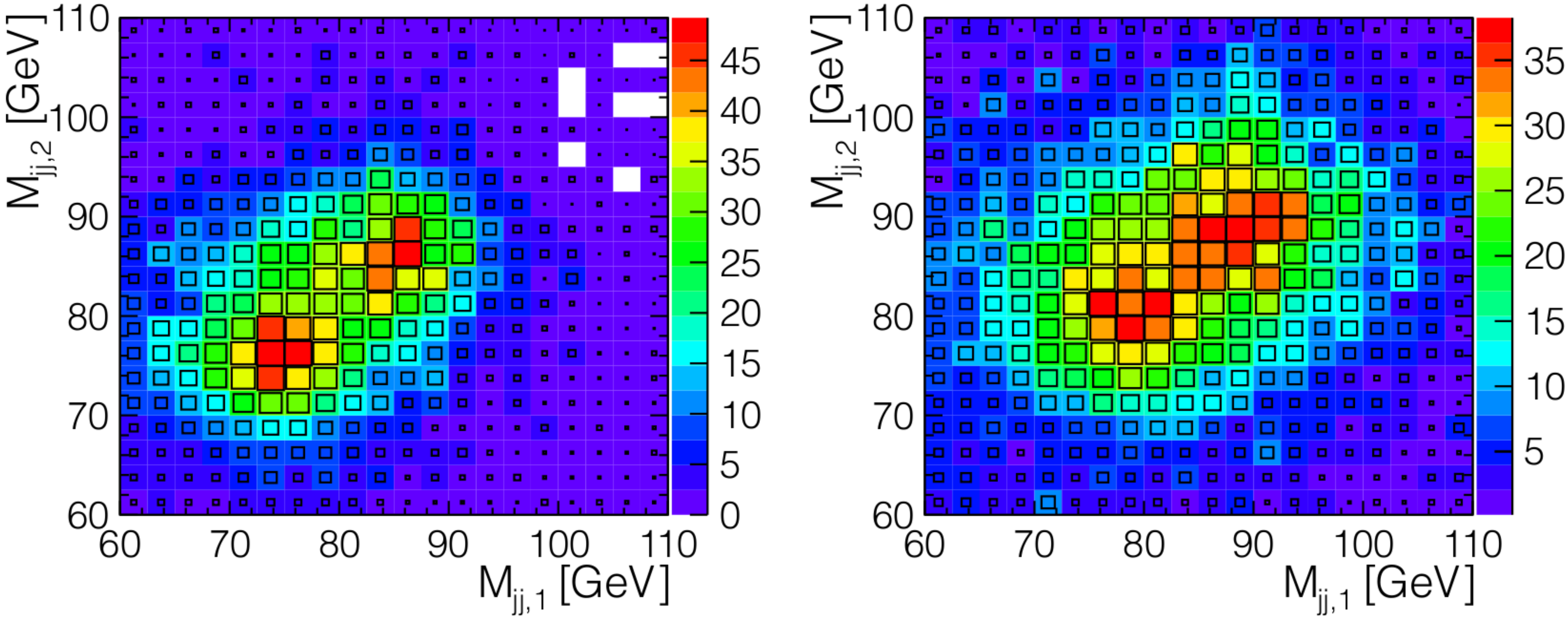

Figure 19: Separation of W and Z from the chargino decay without overlay (left) and with 60 BX of background (right) for CLIC_SiD.

Test of the lepton reconstruction

- Slepton production very clean at CLIC
- SUSY "model II": slepton masses ≈ 1 TeV
- Investigated channels include:

$$e^+e^- \rightarrow \tilde{\mu}_R^+\tilde{\mu}_R^- \rightarrow \mu^+\mu^- \, \tilde{\chi}_1^0\,\tilde{\chi}_1^0$$

$$e^+e^- \rightarrow \tilde{e}_R^+\tilde{e}_R^- \rightarrow e^+e^- \, \tilde{\chi}_1^0\,\tilde{\chi}_1^0$$

$$e^+e^- \rightarrow \tilde{\nu}_e\tilde{\nu}_e \rightarrow e^+e^- W^+W^- \, \tilde{\chi}_1^0\,\tilde{\chi}_1^0$$

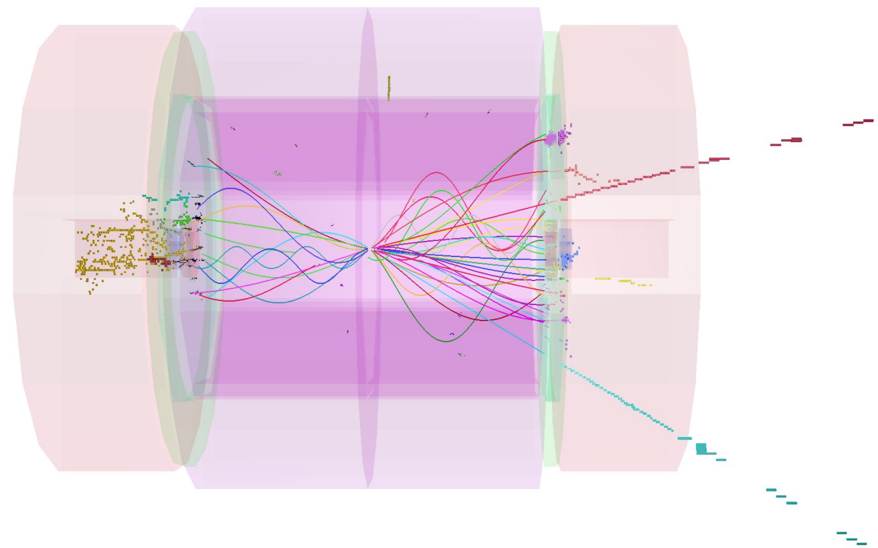

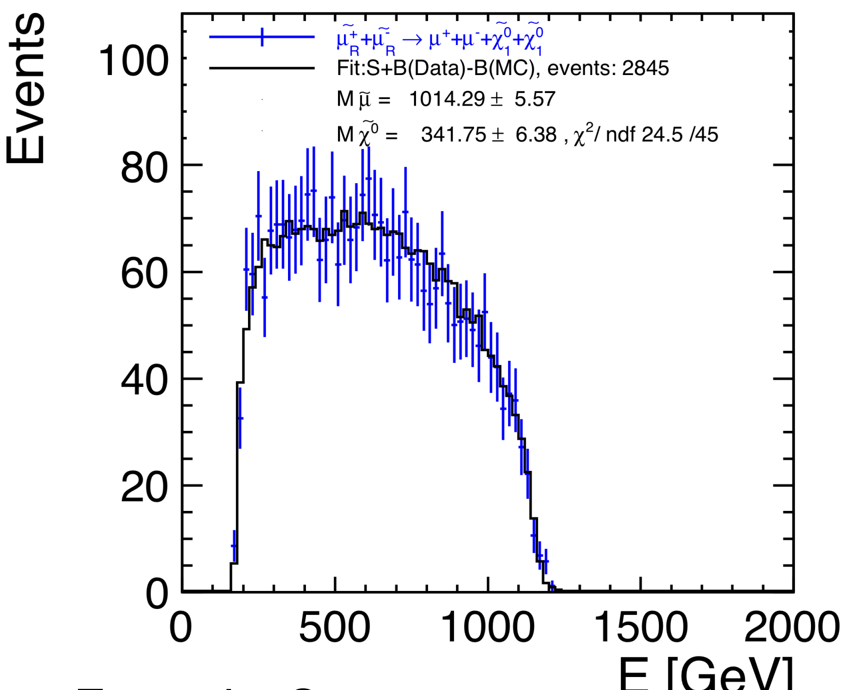

Example: Smuons

- Leptons and missing energy
- Masses from endpoints of energy spectra

$m(\tilde{\mu}_R)$	: $\pm$ 5.6 GeV
$m(\tilde{e}_R)$	: $\pm$ 2.8 GeV
$m(\tilde{\nu}_e)$	: $\pm$ 3.9 GeV
$m(\tilde{\chi}_1^0)$	: $\pm$ 3.0 GeV
$m(\tilde{\chi}_1^\pm)$	: $\pm$ 3.7 GeV

Complex final states

Heavy Higgs bosons:
$e^+e^- \rightarrow HA \rightarrow b\bar{b}b\bar{b}$
$e^+e^- \rightarrow H^+H^- \rightarrow t\bar{b}b\bar{t}$

Flavour tagging crucial!

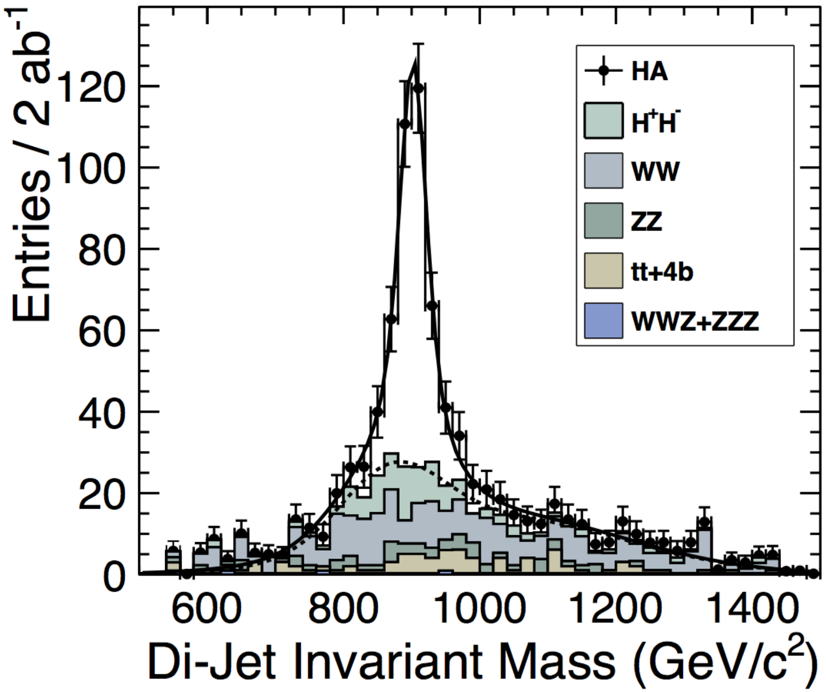

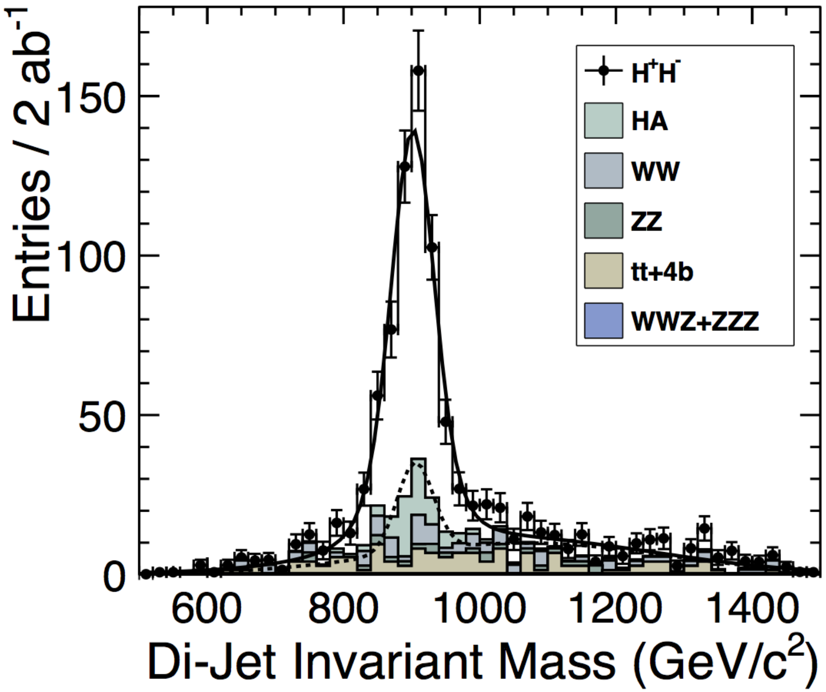

Accuracy of the heavy Higgs mass measurements: ≈ 0.3%